Fisheries and Oceans Canada | Pêches et Océans Canada
Ecosystems and Oceans Science | Sciences des écosystèmes et des océans

Canadian Science Advisory Secretariat (CSAS)

Research Document 2015/005

Pacific Region

The ability of hydrodynamic models to inform decisions on the siting and management of aquaculture facilities in British Columbia

M.G.G Foreman, P.C. Chandler, D.J. Stucchi, K.A. Garver, M. Guo, J. Morrison, D. Tuele

Fisheries and Oceans Canada
Science Branch
3190 Hammond Bay Road
Nanaimo, BC V9T 6N7

April 2015

Canada

Foreword

This series documents the scientific basis for the evaluation of aquatic resources and ecosystems in Canada. As such, it addresses the issues of the day in the time frames required and the documents it contains are not intended as definitive statements on the subjects addressed but rather as progress reports on ongoing investigations.

Research documents are produced in the official language in which they are provided to the Secretariat.

Published by:

Fisheries and Oceans Canada
Canadian Science Advisory Secretariat
200 Kent Street
Ottawa ON K1A 0E6

http://www.dfo-mpo.gc.ca/csas-sccs/
csas-sccs@dfo-mpo.gc.ca

ISSN 1919-5044

Correct citation for this publication:

Foreman, M.G.G., Chandler, P.C., Stucchi, D.J., Garver, K.A., Guo, M., Morrison, J., Tuele, D. 2015. The ability of hydrodynamic models to inform decisions on the siting and management of aquaculture facilities in British Columbia. DFO Can. Sci. Advis. Sec. Res. Doc. 2015/005. vii + 49 p.

TABLE OF CONTENTS

LIST OF TABLES

LIST OF FIGURES

ABSTRACT

Fisheries and Oceans Canada (DFO) is responsible for regulating and managing the aquaculture industry in British Columbia, including the licensing of aquaculture sites and the specification of conditions of licence. To inform regulatory and management decisions, research has been undertaken to better understand the interactions between aquaculture operations and the natural environment by modelling the fate of both passive and biological particles. Two models have been developed for this purpose:

1) an ocean circulation model that hindcasts three-dimensional currents, salinities, temperatures and two-dimensional surface elevations, and
2) a particle tracking model that uses the outputs of the ocean circulation model to simulate the dispersal behaviour of particles released at specific times and locations.

This paper reviews hydrodynamic models currently being used to model ocean circulation in support of aquaculture management, with a focus on the Finite Volume Coastal Ocean Model (FVCOM) and its application to the Broughton Archipelago and Discovery Island regions in British Columbia. Progress in the use of FVCOM to represent the hydrodynamic regime of the two regions includes advances in specifying boundary and forcing conditions; associated challenges are also discussed. The particle tracking models, which use the output of FVCOM, are evaluated by simulating the movement of both passive particles, as well as particles imparted with behaviour and mortality characteristics of sea lice and the Infectious Haematopoietic Necrosis Virus, IHNv.

The caveats and limitations of the application of these models to define aquaculture siting criteria and management zones are discussed. Recommendations for further development work are presented.

Capacité des modèles hydrodynamiques à éclairer les décisions concernant le choix du site et la gestion des installations d'aquaculture en Colombie-Britannique

RÉSUMÉ

Pêches et Océans Canada est responsable de la réglementation et de la gestion de l'industrie aquacole en Colombie-Britannique, ce qui comprend la délivrance de permis aux sites aquacoles et l'imposition de conditions de permis. Dans l'optique d'éclairer les décisions concernant la réglementation et la gestion, des recherches ont été entreprises en vue de mieux comprendre les interactions entre les opérations aquacoles et l'environnement naturel en modélisant ce qu'il advient des particules passives et des particules biologiques. Deux modèles ont ainsi été élaborés à cette fin :

1) un modèle basé sur la circulation océanique qui prévoit a posteriori les courants tridimensionnels, les salinités, les températures et les élévations des surfaces à deux dimensions, et
2) un modèle de suivi des particules qui utilise les produits du modèle basé sur la circulation océanique pour simuler le comportement de dispersion des particules libérées à des moments et à des endroits précis.

Le présent document examine les modèles hydrodynamiques actuellement utilisés pour modéliser la circulation océanique à l'appui de la gestion de l'aquaculture. Il est essentiellement axé sur le modèle de volume fini dynamique des eaux côtières et est appliqué aux régions de l'archipel Broughton et des îles Discovery, en Colombie-Britannique. Les progrès réalisés dans l'utilisation du modèle de volume fini dynamique des eaux côtières pour représenter le régime hydrodynamique des deux régions comprennent les progrès réalisés dans la précision des limites et l'imposition de conditions. Les défis connexes sont également abordés. Les modèles de suivi de particules, qui utilisent les produits du modèle de volume fini dynamique des eaux côtières, sont évalués au moyen de la simulation du mouvement des particules passives et des particules reproduisant le comportement et les caractéristiques liées à la mortalité du pou du poisson et du virus de la nécrose hématopoïétique infectieuse.

Les restrictions et les limitations de l'application de ces modèles pour définir les critères de sélection des sites aquacoles et des zones de gestion sont également abordées. En outre, le présent document renferme des recommandations quant à d'autres travaux d'élaboration de modèles.

1. INTRODUCTION AND BACKGROUND

1.1. BACKGROUND AND MOTIVATION

Fisheries and Oceans Canada (DFO) is responsible for regulating and managing the aquaculture industry in British Columbia (BC). These responsibilities include the licensing of aquaculture sites and the specification of conditions of licence. In addition to conditions respecting the matters set out in subsection 22(1) of the Fishery (General) Regulations, the Minister may specify other conditions in an aquaculture licence including the waters in which aquaculture is permitted (siting) and measures that must be taken to minimize the impact of the operations on fish and fish habitat.

As the primary regulator of the aquaculture industry in BC, DFO recognizes that there are interactions between aquaculture operations and the natural environment. The risks associated with these interactions are considered and addressed through a suite of regulatory tools. Examples include licence conditions that require Fish Health Management Plans (FHMPs) and the application of siting criteria when considering the location of existing and proposed aquaculture facilities.

The siting criteria for marine finfish aquaculture currently applied by DFO were adapted from those previously applied by the Province of British Columbia. These criteria are science-based and have evolved as new information has become available. The application of siting criteria for aquaculture activities is designed to create buffers (proximity or separation distance) in relation to either general, or specific, ecosystem attributes (environmental or socio-economic). The current siting criteria are a set of generic considerations that are applied on a coast-wide basis.

As part of the Department's commitment to evaluating interactions between aquaculture operations and the natural environment in order to inform regulatory and management decisions, research has been undertaken to improve our understanding of the likely behaviour and fate of both passive and biological particles subject to area-specific conditions. Consequently, models have been developed for the purpose of simulating particle dispersion and, in the present context, i) providing estimates of the potential connectivity of finfish aquaculture sites with respect to particle transport, and ii) identifying priorities related to further refinement of the models. Understanding the factors and uncertainties that influence particle dispersal can potentially provide area-specific guidance on the evaluation of current siting criteria and the potential delineation of aquaculture management zones.

Though finfish aquaculture sites are scattered over several sub-regions in southern British Columbia (and a few exist in central coastal waters), hydrodynamic models with sufficient spatial resolution to accurately capture the currents around these sites have only been developed for the Kyuquot Sound, Broughton Archipelago, and Discovery Islands regions (Figure 1). As the Kyuquot model is still being tuned and evaluated, subsequent analyses and conclusions presented in this report are only based on results from the latter two model applications. In both cases there are in fact two models: i) an ocean circulation model that for specific time periods, produces and saves three-dimensional currents, salinities, temperatures, mixing fields and two-dimensional surface elevations; and ii) an offline particle tracking model that reads in these stored fields and uses them to disperse "particles" that are released at specific times and locations. Though the circulation model does include an online particle tracking capability so that both models could be run simultaneously, it is more efficient to calibrate the circulation model first and then store its results at regular intervals so that the particle model can be tuned and run separately. This is because there is no feedback from the

particle model to the circulation model and the latter is more computer intensive and typically requires many runs to calibrate properly

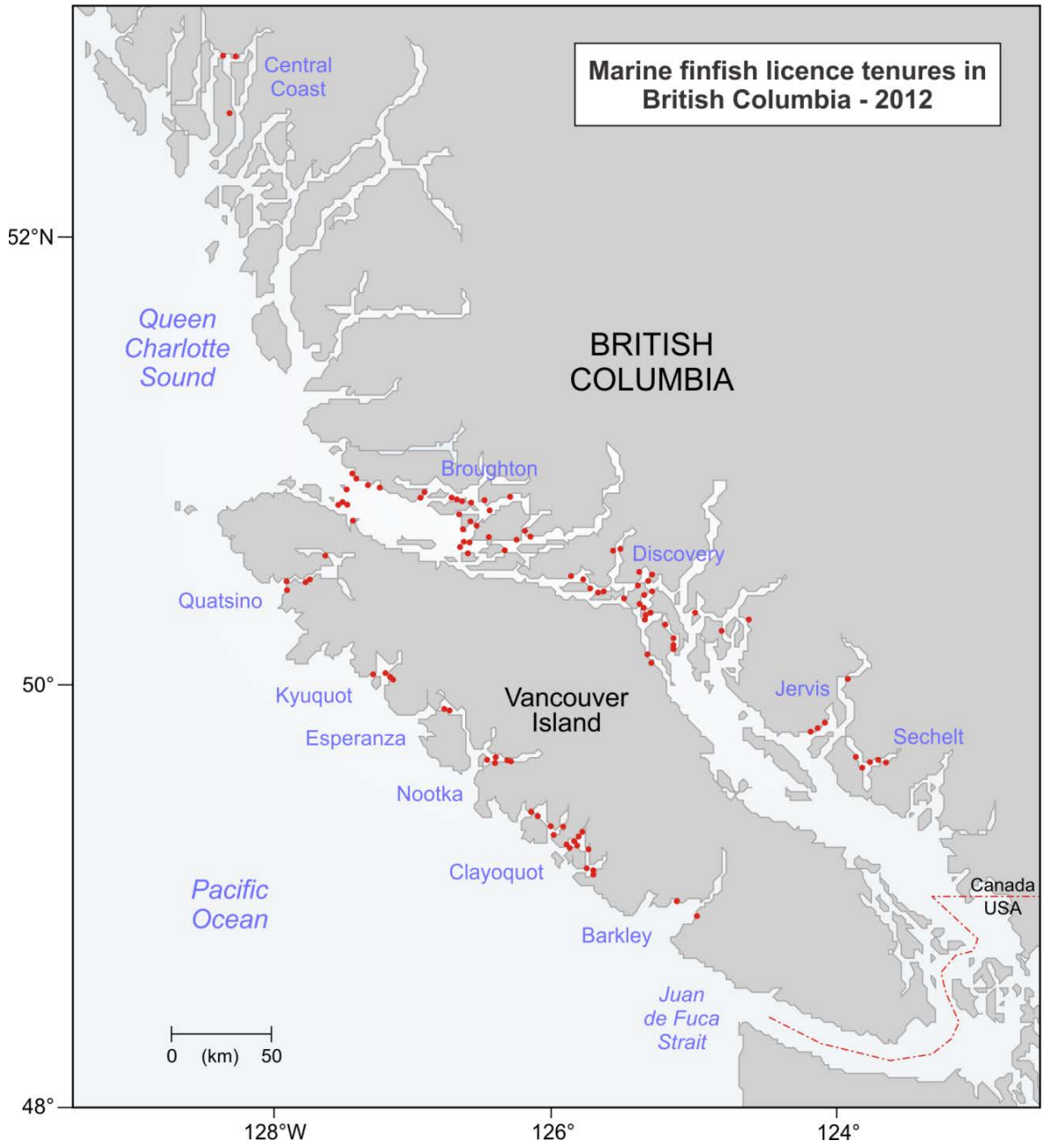

Figure 1. Tenures (red circles) of finfish farms in British Columbia, 2012.

Particles in the tracking model need not be passively floating with the background currents; they can be assigned behaviour (e.g., swimming or sinking capabilities) and/or given biological or chemical attributes that, for example, could simulate life stage progression and mortality dependencies, or degradation into different substances. As such, the particle tracking model can provide an indication of how organisms or pollutants originating on aquaculture sites disperse throughout a region for the time periods when the hydrodynamic model was run. As the currents and water properties vary both spatially and temporally, numerous simulations should be conducted to cover a realistic range of weather and river discharge conditions before

general dispersion conclusions are made. However that may not always be feasible, in light of i) computer and personnel limitations, ii) the availability of the forcing fields (e.g., winds, heat fluxes, river discharges) required by the circulation models, and iii) biological data (e.g., sea lice egg counts on farms, number of diseased fish shedding viruses) required for the particle tracking models. Consequently, there will always be caveats or assumptions associated with any model dispersion results and they are summarized in Section 5.1.

Figure 2. Fish farms (red circles), rivers and place names in the Broughton Archipelago and Discovery Islands regions. SP, HR and CB denote the Sargeaunt Pass, Humphrey Rock, and Cliffe Bay farms referred to later in the text and Figure 8.

Bordered to the south by the Strait of Georgia and to the north by Queen Charlotte Sound, the Broughton Archipelago and Discovery Islands regions (Figure 2) are a complex network of narrow channels and deep fjords whose currents are primarily forced by the winds, freshwater discharges, and the tides. Numerous freshwater inputs within both regions, as well as rivers that enter upstream (e.g., the Fraser River entering the Strait of Georgia) result in background, two-layer estuarine flows (Thomson 1981) which generally move seaward at the surface and in the opposite direction at depth. These currents generally determine the longer-term “particle” transport. However super-imposed on these background flows are tidal and wind-driven currents that for periods of hours to days can have much larger magnitudes and can transport particles in quite different directions. Thus, for example, very strong semi-diurnal tidal currents in Discovery Passage (Canadian Tide and Current Tables 2010) can easily overcome the northward surface estuarine flows and, as will be seen in sections 3.2 and 4.3, advect particles southward into the Strait of Georgia.

In addition to the presence of over 50 salmon-farms, wild salmon species migrate seasonally through both regions en route to, or leaving from, local and more distant (e.g. Fraser River) spawning grounds. Interactions between the farms and wild populations have given rise to environmental concerns (Krkošek et al. 2005, 2007; Brooks and Stucchi 2006; Brooks and

Jones 2008) and a need to better understand the circulation patterns controlling the dispersion of organisms and pollutants originating on the farms. Two issues of particular concern are the dispersion of viruses (e.g., Infectious Haematopoietic Necrosis Virus, IHNv) between farms (Saksida 2006) and between farmed and wild fish (Cohen 2012), and the potential for sea lice originating on farms to adversely impact juvenile salmon migrating from the Fraser (Peterman et al., 2010) and other rivers (Price et al. 2010) to the Pacific Ocean. Such interactions were a major focus in the recent Cohen Commission Report (Cohen 2012) and resulted in several aquaculture recommendations, such as #19 which stated that "on September 30, 2020, the Minister of Fisheries and Oceans should prohibit net pen salmon farming in the Discovery Islands unless he or she is satisfied that such farms pose at most a minimal risk of serious harm to the health of migrating Fraser River sockeye salmon."

1.2. LITERATURE REVIEW OF HYDRODYNAMIC MODELLING FOR AQUACULTURE APPLICATIONS

The application of mathematical models to simulate the hydrodynamics in areas of aquaculture activity has advanced as the need for a better understanding of the physical oceanography in aquaculture management has become clearer. The complexity of the model reflects the complexity of the physical environment it represents and results in the range of hydrodynamic models presently being used today.

The west coast of Canada, and in particular the Broughton Archipelago and Discovery Islands, presents a hydrodynamic regime that is among the most complex in the world for aquaculture use. The large scale physical setting of the British Columbia coast is defined by tectonic forces that have formed, and continue to shape the west coast. Deep fjords, some with shallow sills and many with islands and embayments mix the dense salty oceanic waters with freshwater input from precipitation and snowmelt. Tidal forcing through narrow passages generates flow velocities that can exceed 15 knots (Canadian Tide and Current Tables 2010). There is a seasonal temperature cycle with colder winters and warmer summers separated by spring and fall transition periods. Situated between the Coast Mountains and the northeast Pacific Ocean, the large scale meteorology of the area is dominated by the Aleutian Low Pressure system in winter and the North Pacific High in summer. These two wind regimes can be significantly modified at local scales by the passage of storm fronts, coastal lows, and Arctic outflow conditions. The wind at the sea surface is controlled by the steep sided topography of the fjords steering the air flow in the along-channel direction.

The attributes of the hydrodynamic model suitable for this application include solving equations that conserve momentum in three dimensions in order to characterize velocity and density variations arising from tidal, atmospheric forcing and the mixing of fresh and salt water. This is done by approximating the region of interest with an unstructured triangular grid capable of defining the fine scale details of the coastline and narrow passages and the use of sigma-coordinate (terrain-following) depth layers to accommodate the significant variations in bottom depth. These will all be discussed in more detail in section 2.

A review of the literature of hydrodynamic modelling in support of aquaculture, and specifically net pen finfish farming in a fjord setting, reveals a limited number of models suitable for this purpose. Table 1 summarizes some of their relevant features and is an adaptation of a similar table from the recent comprehensive review of Salama and Rabe (2013). General model characteristics include a horizontal spatial resolution of less than 100 m, representation in the vertical using a sigma-coordinate system with bathymetric smoothing, the use of a minimum depth that avoids the need to incorporate flooding and drying elements, tidal boundary conditions determined from either measured water elevations and flow or from a larger-domain

tidal model, and the requirement to specify fresh water and meteorological (wind stress and heat flux) forcing from either measurements or other modelled output.

Table 1. Primary characteristics of hydrodynamic models used for aquaculture applications (adapted from Salama and Rabe 2013).

	Canada West	**Canada East**	**Norway Hardanger fjord**	**Scotland Firth of Lorn**	**Scotland Loch Linnhe**	**Ireland Mulroy Bay**
Citation	Foreman et al. (2009), Foreman et al. (2012)	Chang et al. (2007), Page et al. (2013),	Asplin et al. (2011)	Adams et al. (2013)	Salama et al. (2013)	Navas et al. (2011)
Model name	FVCOM	FVCOM	ROMS	FVCOM	POLCOM	MOHID
Grid size	50 m-2.3 km (Br) 90 m–1.7 km (Dis)	27 m – 5.7 km (Nfld) 2 5 m – 53 km (NB)	800 m (coastal) 50-200 m (fjord)	70 m – 4.6 km	100 m	50 m
Number of elements	166k (Broughton) 251k (Discovery)	64k (Nfld) 76k (NB)	994x440	25k	365x488	193x244
Maximum model depth [m]	522 (Broughton) 711 (Discovery)	722 (Nfld) 300 (NB)	860	>200	160	47
Number of depths	21	21	35	11	40	5
Flooding/ drying	5 m min depth	yes	no	10 m min depth	no	no
Time step [seconds]	ΔT_E=.075 ΔT_I=.75	ΔT_E=ΔT_I=.72 (Nfld) ΔT_E= ΔT_I=1 (NB)	60	ΔT_E=0.4 ΔT_I=4	15 min	2
Interval of output [h]	1	1	1	1	0.25 - 0.5	1
Boundary	5 tidal	5 tidal	8 tidal	11 tidal	37 tidal	FES2004

	Canada West	Canada East	Norway Hardanger fjord	Scotland Firth of Lorn	Scotland Loch Linnhe	Ireland Mulroy Bay
water level condition	constituents, model and measured	constituents, model and measured	constituents from TPXO model	constituents, European shelf Tidal Inversion model	constituents at local bottom pressure gauge	global tide solution
Fresh water input	(BR) 9 rivers-catchment weights for 6 (DIS);12 rivers catchment weights for 3	none	100 rivers, hydrological model	28 rivers estimated from catchment areas and precipitation rates	6 rivers, catchment weighting from 1 hydrograph	none
Wind input	(BR) - 10 weather stations (DIS) -17 weather stations	1 long term station interpolated to 6 local stations (Nfld) none (NB)	1 km met. model at 3 h time step	Interpolated from 5 weather stations to 20 km grid	NCEP and 6 weather stations	Uniform, based on one weather station
Solar radiation input	Weather stations	none	1 km met model at 3 h time step	Interpolated from 5 weather stations to 20 km grid	none	none

1.3. AN OVERVIEW OF HYDRODYNAMIC MODEL EVALUATIONS

The primary outputs of hydrodynamic models used for aquaculture are three dimensional fields of temperature, salinity, and velocity stored at regular intervals throughout the simulation period. Comparisons between the model output and observations are typically used to evaluate the model results, with the understanding that there are errors in the observations. The output from two models of the same region can be compared to examine differences in model structure or forcing conditions.

There are qualitative and quantitative measures to evaluate the validity of model output. Because observed data are typically constrained to discrete locations and are often limited in duration, an initial evaluation of the modelled output involves a pattern match between the modelled fields and the known circulation characteristics of the study area. Contour mapping of temperature, salinity and velocity can be used to identify areas of the domain or times in the simulation with unrealistic representations.

Where measured data exist, comparisons of modelled and observed scalar parameters, such as temperature, salinity, water elevation or current speed, are made by calculating the root mean square (RMS) difference

$$RMS = \sqrt{\frac{\sum_{i=1}^{n} (X_{m,i} - X_{o,i})^2}{n}} \tag{1.1}$$

where $X_{o,i}$ is the observed value and $X_{m,i}$ is the modelled value at time/place i. Division by the range of the observed data, or by the mean of the observed data provides a normalised root mean square difference. As the agreement between the modelled and measured data improves, the RMS difference decreases.

A scatter plot of observed data versus modelled data is also used to compare the modelled and observed data, with a clustering of points around the 1:1 diagonal an indicator of good agreement. The strength of the relationship between the observed and modelled values can be quantified using a regression analysis to provide a correlation coefficient (r) that increases (up to a value of 1) as variations in the model match variations in the observations. As with the RMS, the correlation analysis sometimes includes a lag in one of the time series to account for systematic biases, like the tidal phases being inaccurate by (for example) one hour. In fact, often the regression will be carried out over a range of lags and leads to determine which produces the highest coefficient value.

$$\mathrm{r} = \frac{\sum_{i=1}^{N} \left(X_{o,i} - \overline{X}_{o,i}\right)\left(X_{m,i} - \overline{X}_{m,i}\right)}{\sqrt{\sum_{i=1}^{N} \left(X_{o,i} - \overline{X}_{o,i}\right)^2} \sqrt{\sum_{i=1}^{N} \left(X_{m,i} - \overline{X}_{m,i}\right)^2}} \tag{1.2}$$

The degree to which deviations of the observations about their mean correspond to the deviations of the modelled output about the observed mean is a measure of the model skill; perfect agreement gives a skill of 1 and no agreement a skill of 0. This is also termed the index of agreement.

$$\mathrm{skill} = \text{ index of agreement} = 1 - \frac{\sum_{i=1}^{N} \left|X_{m,i} - X_{o,i}\right|^2}{\sum_{i=1}^{N} \left(\left|X_{m,i} - \overline{X}_{o,i}\right| + \left|X_{o,i} - \overline{X}_{o,i}\right|\right)^2} \tag{1.3}$$

Because tidal forcing in fjords can be a significant contributor to the current regime, an evaluation of the tidal component is a good indicator of how well the model represents the barotropic circulation. The amplitude and phase of the M_2 and K_1 constituents are typically analysed as they are the largest contributors to energy in the semidiurnal and diurnal frequency bands and their accuracy is usually representative of other constituents in those bands. The distance, D, in the complex plane provides a measure of agreement, with a value of 0 signifying perfect agreement.

$$\mathrm{D} = \sqrt{\left(A_0 \cos g_0 - A_m \cos g_m\right)^2 + \left(A_0 \sin g_0 - A_m \sin g_m\right)^2} \tag{1.4}$$

where $A_o, A_m, g_o, g_m,$ are the observed and modelled amplitudes and phases, respectively. This analysis can be applied to either the sea surface elevation or a one-dimensional component (e.g., along-channel) of the current.

The relative error between observed and modelled values of the two-dimensional current can be expressed as the velocity difference ratio VDR, where better agreement is reflected as a lower VDR.

$$\mathrm{VDR} = \frac{\sum_{i=1}^{N} \left| V_{m,i} - V_{o,i} \right|^2}{\sum_{i=1}^{N} \left| V_{o,i} \right|^2} \tag{1.5}$$

where $V_{o,i}$ and $V_{m,i}$ are the observed and modelled velocity vectors, respectively.

The validation process evolves as the hydrodynamic model is developed and calibrated. The validation methods described above can each be used based on how well the model output is able to fulfill the purpose at hand, such as particle tracking, sea lice survival, or virus concentrations. Comparing measures of agreement with models in other regions is not straightforward as each model domain presents its unique challenges which will affect how well the model can simulate the environmental conditions of that specific region. Of greater significance is the ability of the model to provide three dimensional fields of salinity, temperature and current that can be used to accurately represent conditions where there are no direct observations. With sufficient skill the model can progress from hindcasting conditions when and where observations are available, to providing realistic simulations of conditions with no observed data, to eventually simulating conditions where predicted values of meteorological and freshwater forcing are used to drive the model.

2. OVERVIEW AND EVALUATION OF THE HYDRODYNAMIC MODEL

2.1. OVERVIEW OF THE HYDRODYNAMICS AND FVCOM

The modelling carried out in both the Broughton and Discovery regions employs the Finite Volume Coastal Ocean Model (FVCOM) developed by Chen et al. (2003, 2004, 2006ab). FVCOM solves the three-dimensional (3D) primitive equations for velocity and surface elevation and 3D transport/diffusion equations for salinity and temperature in the presence of turbulent mixing. In Cartesian coordinates, these equations are (Chen et al. 2011)

$$\frac{\partial u}{\partial t} + u\frac{\partial u}{\partial x} + v\frac{\partial u}{\partial y} + w\frac{\partial u}{\partial z} - fv = -\frac{1}{\rho_o}\frac{\partial (p_H + p_a)}{\partial x} - \frac{1}{\rho_o}\frac{\partial q}{\partial x} + \frac{\partial}{\partial z}(K_m \frac{\partial u}{\partial z}) + F_u \tag{2.1}$$

$$\frac{\partial v}{\partial t} + u\frac{\partial v}{\partial x} + v\frac{\partial v}{\partial y} + w\frac{\partial v}{\partial z} + fu = -\frac{1}{\rho_o}\frac{\partial (p_H + p_a)}{\partial y} - \frac{1}{\rho_o}\frac{\partial q}{\partial y} + \frac{\partial}{\partial z}(K_m \frac{\partial v}{\partial z}) + F_v \tag{2.2}$$

$$\frac{\partial w}{\partial t} + u\frac{\partial w}{\partial x} + v\frac{\partial w}{\partial y} + w\frac{\partial w}{\partial z} = -\frac{1}{\rho_o}\frac{\partial q}{\partial z} + \frac{\partial}{\partial z}(K_m \frac{\partial w}{\partial z}) + F_w \tag{2.3}$$

$$\frac{\partial u}{\partial x} + \frac{\partial v}{\partial y} + \frac{\partial w}{\partial z} = 0 \tag{2.4}$$

$$\frac{\partial T}{\partial t} + u\frac{\partial T}{\partial x} + v\frac{\partial T}{\partial y} + w\frac{\partial T}{\partial z} = \frac{\partial}{\partial z}(K_h \frac{\partial T}{\partial z}) + F_T \tag{2.5}$$

$$\frac{\partial S}{\partial t}+u\frac{\partial S}{\partial x}+v\frac{\partial S}{\partial y}+w\frac{\partial S}{\partial z}=\frac{\partial}{\partial z}(K_h\frac{\partial S}{\partial z})+F_S \quad (2.6)$$

$$\rho = \rho(T, S, p) \quad (2.7)$$

Where x, y, and z are the east, north, and vertical axes in the Cartesian coordinate system; u, v, and w are the x, y, z velocity components; T is the temperature; S is the salinity; ρ is the density; p_a is the air pressure at sea surface; p_H is the hydrostatic pressure; q is the non-hydrostatic pressure; f is the Coriolis parameter; g is the gravitational acceleration; K_m is the vertical eddy viscosity coefficient; and K_h is the thermal vertical eddy diffusion coefficient F_u, F_v, F_w, F_T, and F_S represent the horizontal and vertical momentum, thermal, and salt diffusion terms. The total water column depth is $D=H+\zeta$, where H is the bottom depth (relative to $z = 0$) and ζ is the height of the free surface (relative to $z = 0$). $p = p_a + p_H + q$ is the total pressure, in which the hydrostatic pressure p_H satisfies

$$\frac{\partial p_H}{\partial z}=-\rho g \Rightarrow p_H=\rho_o g\zeta+g\int_z^0 \rho\, dz' \quad (2.8)$$

These equations are solved subject to specific surface, bottom, and lateral boundary conditions and the interested reader is referred to the FVCOM manual (Chen et al. 2011) for details.

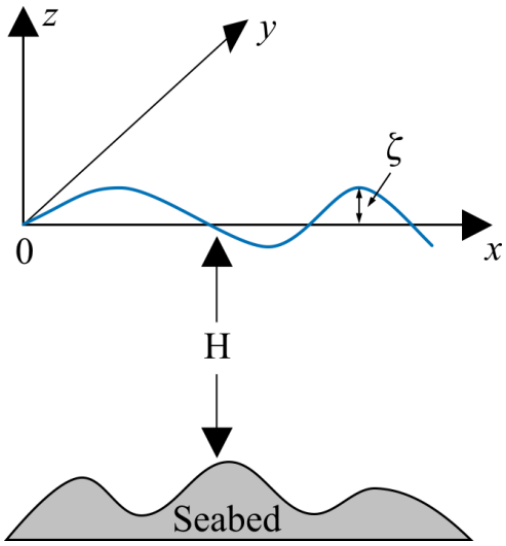

Figure 3. Illustration of the orthogonal coordinate system: x: eastward; y: northward; z: upward. (adapted from Chen et al., 2011).

Numerical analysis techniques must be first used to approximate and then solve the primitive equations on a computer. Numerous methods have been developed over recent decades and are usually categorized into two groups; those which divide the oceanic region of interest into a grid of rectangles and those that instead choose other polygons, typically triangles. FVCOM falls into the latter category and the interested reader is referred to Chen et al. (2011) for details on the particular numerical approximations it employs.

It is important to note that there are underlying assumptions within the primitive equations that may limit their ability to describe all types of oceanic circulation problems. The first is that the water is assumed to be incompressible and Boussinesq, meaning that variations in water density are important when considering buoyancy but too small to affect the inertial terms in the

equations of motion. As a consequence, sound waves and the thermal expansion of ocean water due (for example) to climate warming, cannot be captured with the primitive equations. The second is the hydrostatic approximation in which vertical accelerations are assumed to be small compared to gravitational acceleration and the pressure at any point in the ocean is only due to the weight of the water above it. With respect to the foregoing equations, use of the hydrostatic assumption means ignoring the non-hydrostatic pressure (setting *q=0*) and not being able to accurately represent dynamics involving highly convective flows or internal waves (such as are generated around the sill in Knight Inlet). (That said, there is a yet-untested, non-hydrostatic version of FVCOM that claims to capture these dynamics.) Finally, assumptions and parameterizations in both the vertical (i.e., K_m in equations 2.1, 2.2, 2.3) and horizontal mixing terms in the primitive equations are topics of ongoing research (both in terms of understanding the physics and representing the processes numerically) and as such, may not capture the actual mixing processes accurately.

The domain over which FVCOM solves the primitive equations is covered with a variable resolution triangular grid, as opposed to the rectangular grids used in finite difference models like Masson and Fine (2012). This allows much more flexibility in representing regions with complicated coastlines and bathymetric features such as those found along the BC continental shelf. From a numerical analysis perspective, smaller triangles should mean a more accurate solution of the underlying partial differential equations (2.1 to 2.7 above). However, smaller triangles not only necessitate smaller time steps in order to maintain model stability, but also increase the total number needed to cover the desired region. Both these factors make for longer computation times. Consequently, the choice of grid resolution is often determined by available computer resources, rather than triangle sizes that are deemed necessary to resolve important features with sufficient accuracy. That said, unstructured grid models like FVCOM do offer the flexibility of increasing the grid resolution in certain regions of high interest and allowing it to be much coarser in other regions of less interest, thereby saving additional computational costs that would be incurred if the resolution were similar everywhere.

There are several software packages (e.g., Henry and Walters 1993) that can be used to create these triangular grids. As input they typically require digitized coastline and bathymetry information, data that for the Broughton and Discovery regions are obtainable from the Canadian Hydrographic Service (CHS). Though bathymetric data were often sparse in the past, new technology like multi-beam sonar is capable of providing values with horizontal resolutions around 2 m which is finer than that needed by the models. In such cases, some sort of averaging is necessary. The shape of the triangles can impact the accuracy of the numerical solutions (e.g., Foreman 1984) and a general rule is to avoid angles less than 30° and make the triangles as close to equilateral as possible. Rapid transitions in size can also cause numerical problems (energy trapping), so it is also best to have gradual changes from coarse to fine. In the vertical, the horizontal triangles are extended straight downward from the surface to the seabed. Then each column is divided into a prescribed number of terrain-following vertical layers, as seen in Figure 4. Though there is the same number of layers everywhere, they need not be equally spaced and FVCOM offers various options for their definition. Typically, they are chosen to have finer resolution near the surface and bottom so as to better capture those boundary layers. However, as there can be numerical problems if the bathymetry changes too quickly within an element (Haney, 1991), it is customary to smooth the bathymetry. This issue is discussed in more detail in Foreman et al. (2012).

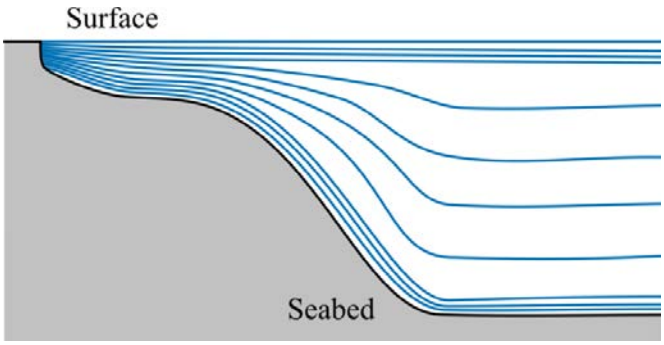

Figure 4. An example of vertical layers in FVCOM (adapted from Chen et al. 2011).

FVCOM can be forced with any combination of tides, wind, river runoff, surface heating, and open ocean inflows. Though it can be run with one or more coupled modules (e.g., nutrient-phytoplankton-zooplankton, surface wave, and sediment transport), they are not employed here. The code is written in Fortran and structured to take advantage of Message Passing Interface (MPI) so that it can be run on multi-processor machines such as the High Performance Computers at the Institute of Ocean Sciences and Bedford Institute of Oceanography. FVCOM has also been adopted as the preferred unstructured grid modelling tool to be used by the Nearshore Sub-Group within the DFO Centre of Expertise COMDA (Centre for Ocean Model Development and Application). As such, it has a user group within Canada, as well as the much larger international community, to rely on for advice and experience.

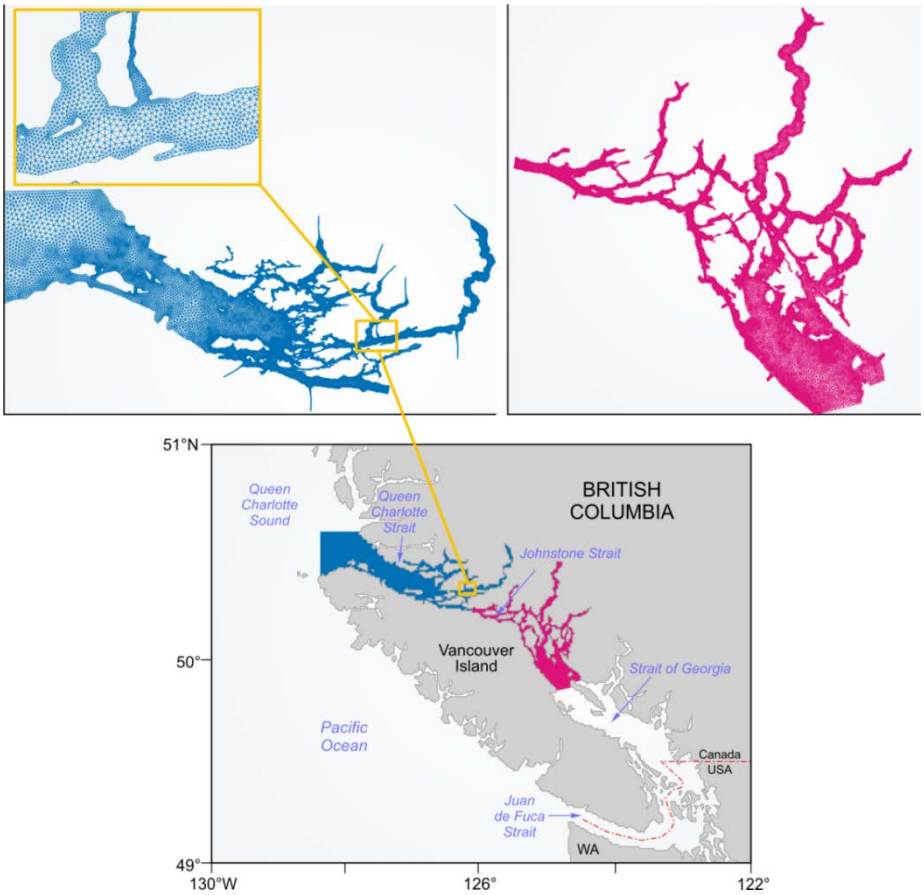

Figure 5. The fine resolution Broughton Archipelago grid (blue) with a close-up around the Knight Inlet and Tribune Channel confluence (yellow box), and the coarse Discovery Islands grid (red).

As mentioned above, FVCOM-based circulation and biological models have been developed for the Broughton Archipelago and Discovery Island regions (Foreman et al. 2006; Foreman et al. 2009, Stucchi et al. 2011, Foreman et al. 2012). The original Broughton grid had approximately 43,000 nodes and a spatial resolution that was seldom smaller than 200 m while the newer version (Figure 5) has approximately 98,000 nodes and a spatial resolution as small as 50 m near the farms. The present Discovery grid (Figure 5) has approximately 36,000 nodes and a coarser resolution (approximately 100 m at its finest), though a refined version (134,000 nodes) with resolution down to 50 m is presently being tested.

2.2. FVCOM FORCING AND INITIAL FIELDS

FVCOM requires three-dimensional temperature and salinity fields as initial conditions and these are typically computed by interpolating and smoothing (Foreman et al. 2008) a combination of historical and recent CTD (conductivity, temperature, depth) observations which may, or may not have, adequate spatial and temporal coverage. Atmospheric, tidal, river discharge, and lateral boundary fields are also required to force the circulation models when hindcast simulations are required for specific periods of time.

Tidal forcing is typically restricted to the largest 5-8 constituents as they account for approximately 60-85% of the tidal range in the diurnal and semi-diurnal frequency bands. The addition of another 10-20 constituents might raise this total to 95% but that is generally not done as subsequent analyses to assess the accuracy of the additional constituents would require simulations of at least six months. The tidal forcing is imposed as specified elevations (constituent amplitudes and phases) at the open ocean boundaries and this information is generally available from a combination of analyses of historical tide gauge records, and/or results from tidal models covering a larger domain. No flow is permitted normal to the coastal boundaries and to-date the wetting-and-drying capability within FVCOM (that allows for mudflats at low tide) has not been implemented. Rather, a minimum depth of 5 m has been imposed throughout both model domains so that even at extreme low tides, all grid elements remain wet. The Broughton and Discovery regions generally have steep sided coastlines so this was felt to be a reasonable approximation (unlike the Bay of Fundy, for example, where wetting and drying is necessary).

Where available, freshwater discharge data were obtained from the hydrometric network maintained by Environment Canada (EC). In the Broughton, these data are available for Klinaklini, Wakeman, Kingcome, Nimpkish, Salmon and Tsitika Rivers (Figure 2) and were extrapolated to the Glendale, Ahta and Kakweikan Rivers by comparing watershed areas, as described in Foreman et al. (2006). In the Discovery, these data are only available for the Homathko, Salmon, Campbell, and Oyster Rivers (Figure 2) and similar estimates were made for the Powell, Toba, Brem, Southgate, Estero, Phillips, Apple, and Stafford Rivers. FVCOM also requires the salinities and temperatures of these discharges. The former are usually set to zero while the latter, rarely available from direct in-river observations, are typically estimated from nearby surface CTD observations.

Given the scarcity of EC (and other) weather stations and the absence of atmospheric models with sufficient resolution to adequately capture variations dictated by the mountainous terrain in both regions, the specification of atmospheric forcing posed a considerable challenge. Using an extensive array of moored and profiling currents meters in Knight Inlet, Baker and Pond (1995) found a high correlation between winds and surface flows over two month-long periods in 1988 and 1989, thereby demonstrating that the wind does play an important role in the regional circulation. In order to overcome this weather deficiency, a network of stations was installed throughout the Broughton Archipelago in May 2007 and the Discovery Islands in April 2010. Though there have been a few relocations and re-deployments necessitated by either too much

sheltering or storms knocking down the towers, the stable network of 9 and 14 stations shown in Figure 6 (including the EC stations at Port Hardy and Campbell River airports and a few stations at fishing resorts) have generally produced usable observations since those times. Due to impending funding cuts, the original Broughton stations were removed in early 2010. But with the inception of the Broughton Archipelago Monitoring Project, new stations were purchased by Marine Harvest Canada (MH), deployed at the same locations later that year, and have been maintained cooperatively by MH and DFO since that time.

Interpolating/extrapolating these wind observations to all the model grid elements in a manner that accounts for orographic steering by the mountainous terrain is a nontrivial exercise. After a few unsatisfactory attempts, we eventually settled on either i) a thin-plate spline technique (Wahba 1990) with the insertion of pseudo-stations to account for coastal topography or, ii) assimilating the observations into a simplified atmospheric model with the representer approach of Bennett (2002). (See Foreman et al. (2009) for more details.) The accuracy of the wind fields arising from both approaches is not only limited by various choices within the numerical techniques themselves, but also by the representativeness of the observations (e.g., the siting may not accurately capture winds from certain directions), and their availability (data gaps due to a variety of malfunctions were not uncommon). Studies that attempt to fill these gaps via correlations with the observations from nearby or permanent stations (e.g., those from the Port Hardy and Campbell River airports) have been carried out with some success. However, a better long term strategy would be the development of a high resolution atmospheric model with either full or simplified (e.g., Hayco 2010) dynamics. See section 5.3g) for further discussion.

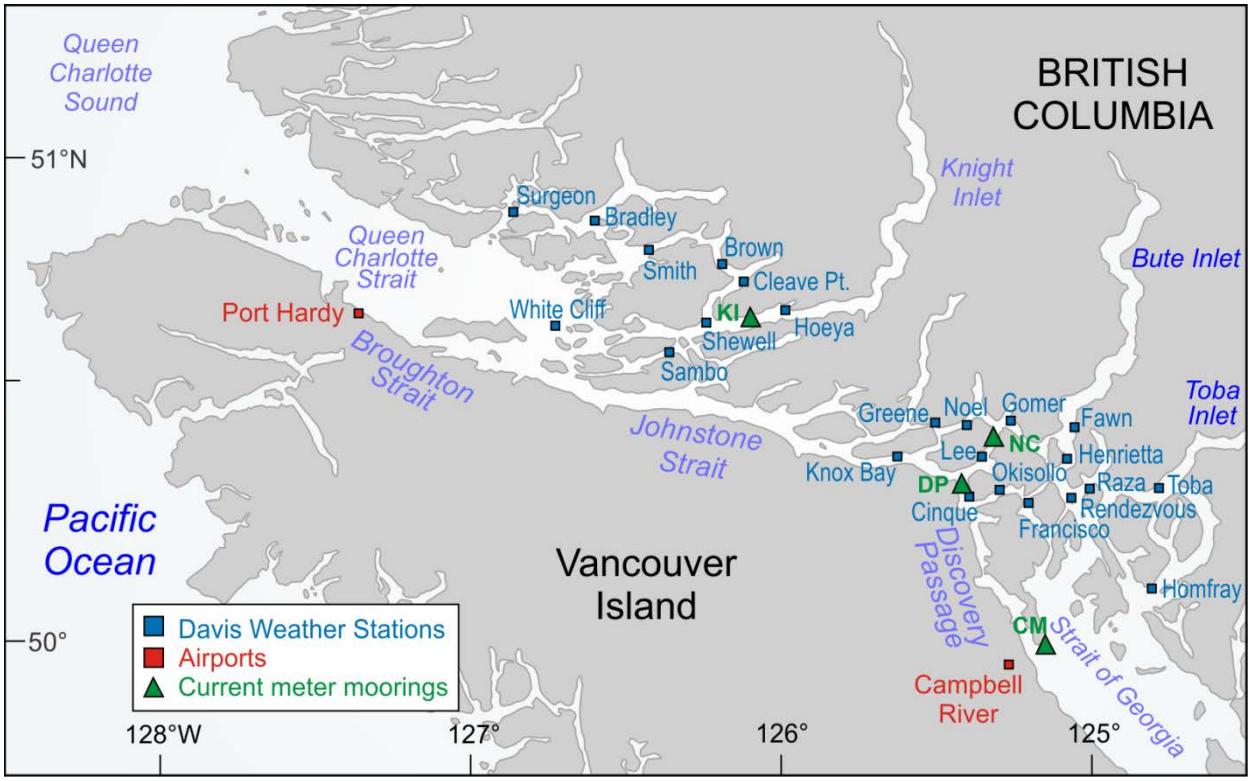

Figure 6. Weather stations and ADCP current meter mooring locations in the Broughton and Discovery regions. KI denotes the Knight Inlet mooring, results are shown in Figure 7; NC, DP, and CM denote the Discovery moorings, results are shown in Figure 10.

2.3. RESULTS FROM, AND EVALUATIONS OF, THE BROUGHTON AND DISCOVERY HYDRODYNAMIC MODELS

As results from, and evaluations of, the Broughton and Discovery hydrodynamic models have been previously reviewed and are presented in Foreman et al. 2009 and Foreman et al. 2012, only examples will be presented here. In both cases, hindcast simulations were carried out for relatively short periods of time (March 13 to April 3, 2008 for the Broughton and April 1 to April 28, 2010 for the Discovery) as at the time of those publications, there were only adequate forcing fields and in situ current observations available for those periods. Both these hindcasts neglected heat flux forcing as observed air and water temperatures are generally close at those times of year and solar radiation input is minimal due to low solar zenith angles and heavy cloud cover. Since those two publications, more simulations have been carried out. In the Broughton, hindcasts have been run for:

i. May 1 - 22, 2008

ii. May 10 - 31, 2010

iii. March 1 to July 31, 2009

In the Discovery region, model runs have been completed for the April 29 to October 31, 2010 period. Surface heat flux forcing was included in all these more recent runs, and this meant repeating the April 2010 Discovery run of Foreman et al. (2012). In the Broughton case, the model grid was also refined to provide more resolution in the region of the farms. However, heavy time commitments to other projects meant that there has yet to be an extensive evaluation of any of these new model results against available current meter, and/or farm salinity and temperature observations.

As a sample evaluation of the Broughton hindcast (with the coarse grid) for March 2008, Figure 7 compares model along-channel currents at 4.5 m depth with those measured by an ADCP moored in lower Knight Inlet (KI as shown in Figure 6). The along-channel components of the measured and model winds at the nearby Hoeya weather station are also included to provide a visual correlation of the effect that storms have on these near surface flows and to further assess the accuracy of the wind interpolation technique. Notice that the strong eastward winds on March 16 are slightly underestimated by the model, and for a few time periods when these winds were not available, the values inserted by the interpolation method produced events that appear to be inconsistent with measured winds on either side of the interruption. Winds and observed currents during the model spin-up period of about 3 days (the model forcing was ramped up over 2.5 days) have been included to show that there were no usual events (i.e., storms) whose after-effects might affect the observed but not model currents. After this initial model spin-up, the observed and model currents are seen to show reasonable agreement. Both time series have tidal oscillations of almost 20 cm s^{-1} superimposed on an average westward surface (negative) flow of 20-25 cm s^{-1}, consistent with the estuarine conditions that were observed previously in Knight Inlet. Though the March 16 strong eastward winds are seen to produce a notable response in both the observed and modelled 4.5 m flows, later and weaker storms such as those on March 18, 21, and 23 are seen to have much less impact. The model simulation was repeated with no wind forcing and those flows are also shown in Figure 7. Further substantiating the conclusions of Baker and Pond (1995), they are clearly less accurate than those that included wind forcing, not only missing the effects of the March 16 storm but also showing a generally weaker eastward background flow.

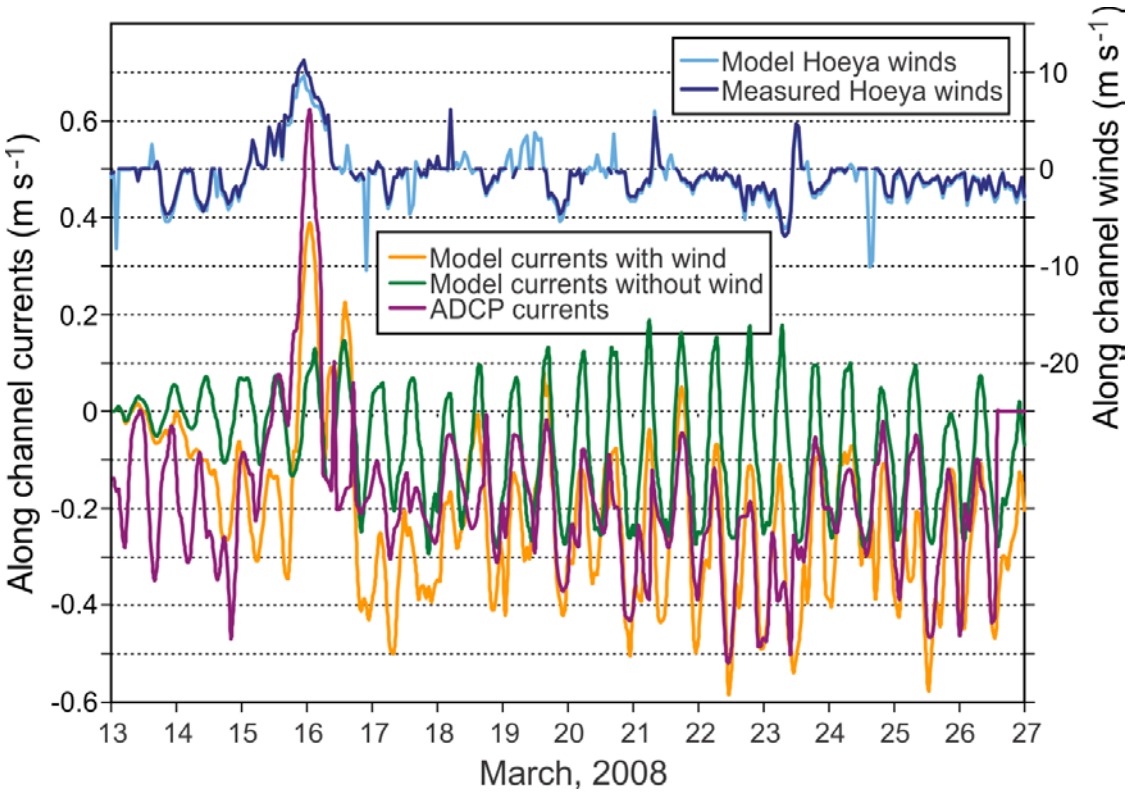

Figure 7. Along-channel model and observed currents at 4.5 m depth at a Knight Inlet mooring (KI in Figure 6), and along-channel winds at the nearby Hoeya weather station (Figure 6), for the period of March 13 to 26, 2008. Positive winds and currents are directed 15° north of eastward.

Average D values (equation 1.4) for the M_2 and K_1 tidal constituents at eight tide gauge locations were 5.8 cm and 2.7 cm, corresponding to errors of approximately 4.2% and 5.3%, respectively. Correlation coefficients (equation 1.2) between model and observed along-channel currents at six moorings demonstrated that the model deep currents were generally more accurate than those near the surface. Specifically, the correlation coefficients for currents at depths below 50 m were consistently higher than 0.72 while those for currents in the top 20 m ranged between 0.47 and 0.84. These depth-dependent differences are to be expected as near surface variability is more strongly determined by the winds whereas variability at depth arises predominantly from the tides. Also, the tidal forcing was specified with a high degree of accuracy whereas there were larger uncertainties with the wind forcing that undoubtedly influenced the accuracy of the modelled near surface currents. Further comparisons between along-channel M_2 amplitudes and phases arising from harmonic analyses of model and observed currents at moorings deployed prior to 2008 demonstrated generally good agreement – the major exceptions being in channels where bathymetric smoothing within the model made the deepest sections shallower and the model currents stronger. The mean flows at these same locations displayed similar accuracy.

As mentioned earlier, without a high resolution atmospheric model for the region it is difficult to provide accurate wind forcing for FVCOM at all points in the model domain. Though the nine weather stations that were installed to augment the one permanent station at Port Hardy airport certainly improved the definition of the wind field, choices in site selection due to the heavily forested terrain and steep-sided coastlines meant that the data from some sites had a directional bias due to partial sheltering of winds from particular directions. Although a credible data assimilation technique was devised for interpolating and extrapolating the observed winds

to the entire grid, missing and questionable data, and assumptions associated with the assimilation technique, undoubtedly meant that some regions in the model domain had more accurate wind forcing than others.

Though temperature and salinity values for the March 2008 simulation period were in general not sufficiently variable to provide a good indication of model performance, root mean square differences between near surface water temperatures observed at five aquaculture sites and those computed by the model were consistently less than 1°C suggesting reasonable accuracy. Analogous salinity differences computed at the two farms with sufficiently accurate instrumentation were larger (up to 2.7 psu at one farm) and possibly due to a combination of inaccurate discharges (estimated from nearby gauged rivers) and inaccurate winds transporting the river plume which will influence the salinity on a more local space scale than temperature. More extensive details of the Broughton hindcast evaluation can be found in Foreman et al. (2009).

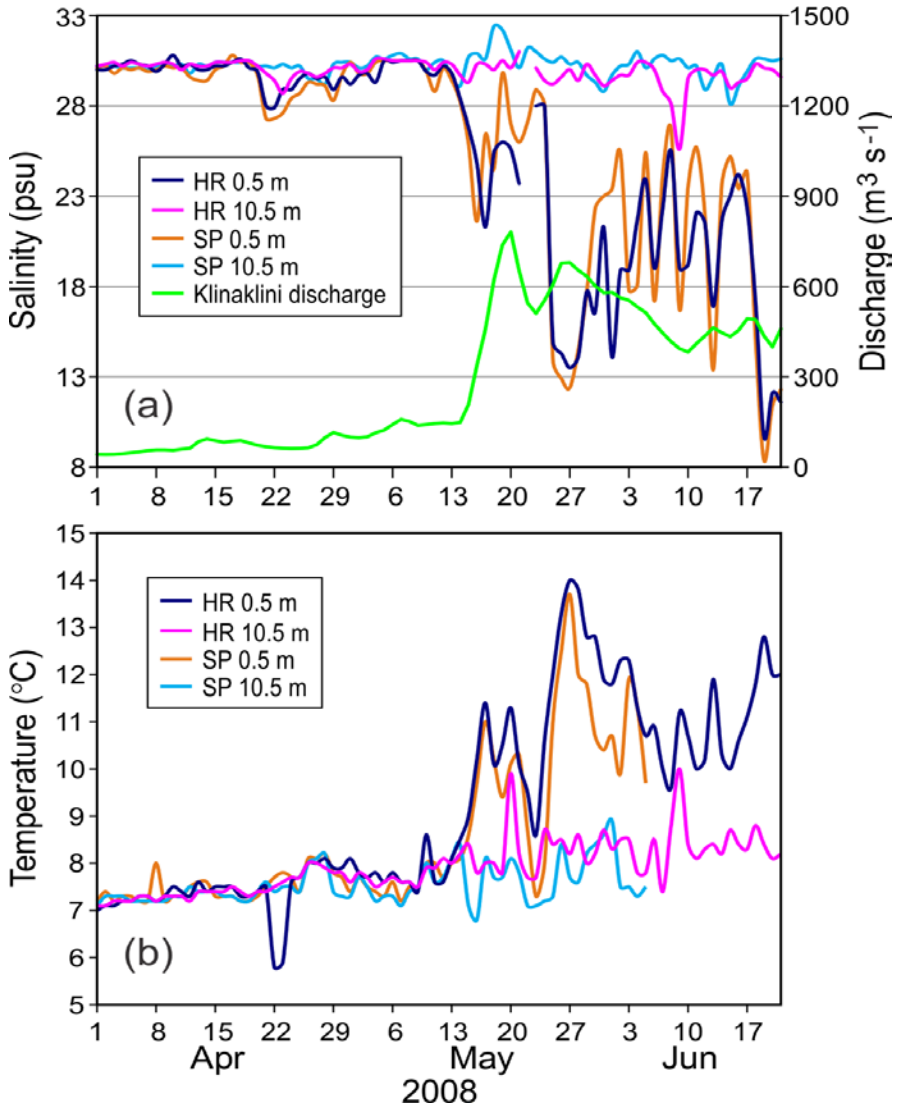

Figure 8. a) Spring 2008 Klinaklini River discharges and salinity time series at 0.5 and 10.5 m depth at the Sargeaunt Pass (SP) and Humphrey Rock (HR) fish farms (Figure 2), b) corresponding temperatures at SP and HR.

As mentioned above and described in more detail in Stucchi et al. (2011), temperature and salinity play important roles in sea lice development and mortality. Egg viability decreases and nauplii mortality increases with lower salinity while both egg production time and the time between nauplii life stages decrease with rising temperature. Thus the accuracy with which temperature and salinity are estimated in the circulation model can have significant impact on the subsequent copepodid concentrations estimated in the biological particle tracking model, to be described in more detail in section 4.2. Although the changing near-surface temperature and salinity conditions between March and May (e.g. Figure 8) would appear to have opposing effects on copepodid concentrations, Brooks (2005) used historical conductivity-temperature-depth (CTD) data from the Broughton region to hypothesize that reduced salinity provides a natural control of sea lice during summer months.

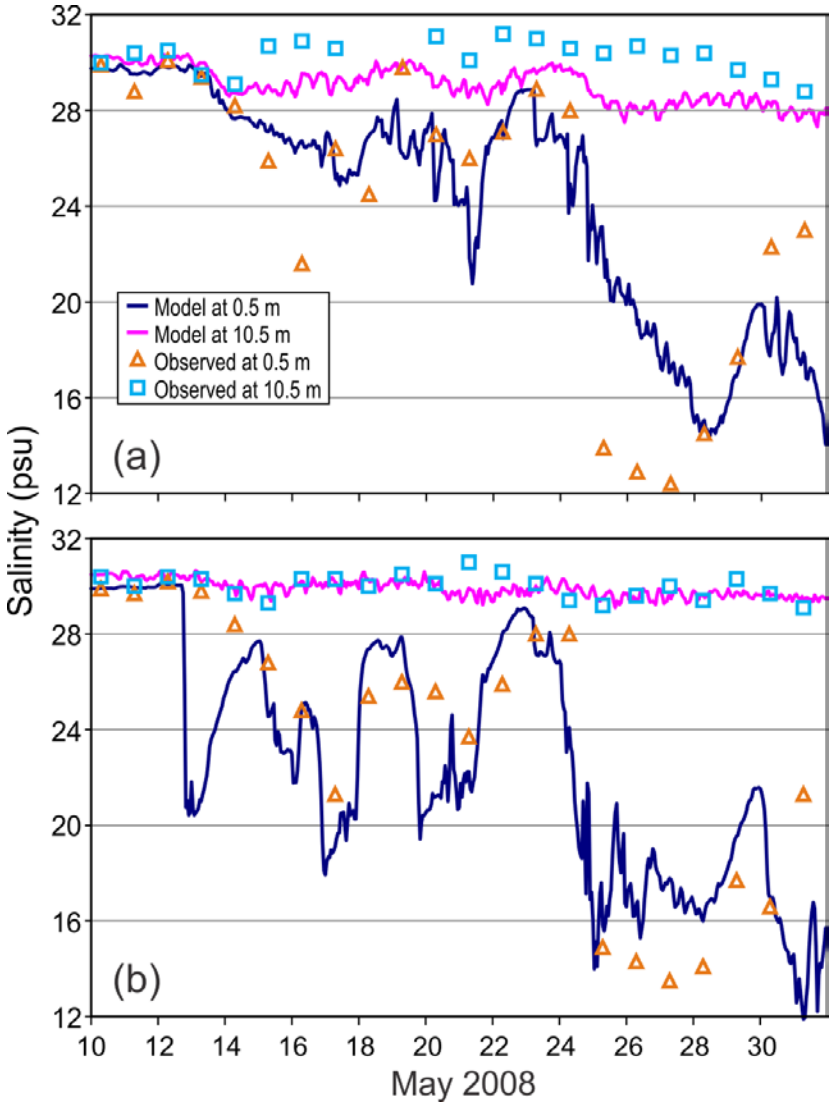

Figure 9. Modelled and observed salinity time series for the period of May 10 to May 31, 2008 at the a) Sargeaunt Pass and b) Humphrey Rock fish farms (Figure 2).

Figure 9 shows observed and modelled salinity time series at 0.5 and 10.5 m depth at the Sargeaunt Pass and Humphrey Rock farms. The observations were taken only once a day, generally at around 8:00am, so unlike the model values, tidal oscillations may be aliased. Though the model salinities at 0.5 m have not captured all the observed variability, there is

reasonable agreement during the May 20 and May 24 mixing events and the re-stratification period of May 25-28. Model accuracy is somewhat better at SP than HR and this is probably explained by the fact that the winds, and thus currents, are more accurate in Knight Inlet than Tribune Channel. The salinities at 10.5 m show little variation with the winds (and tides) and discrepancies between the model and observed values can, in all likelihood, be traced back to inaccuracies in the model initial conditions.

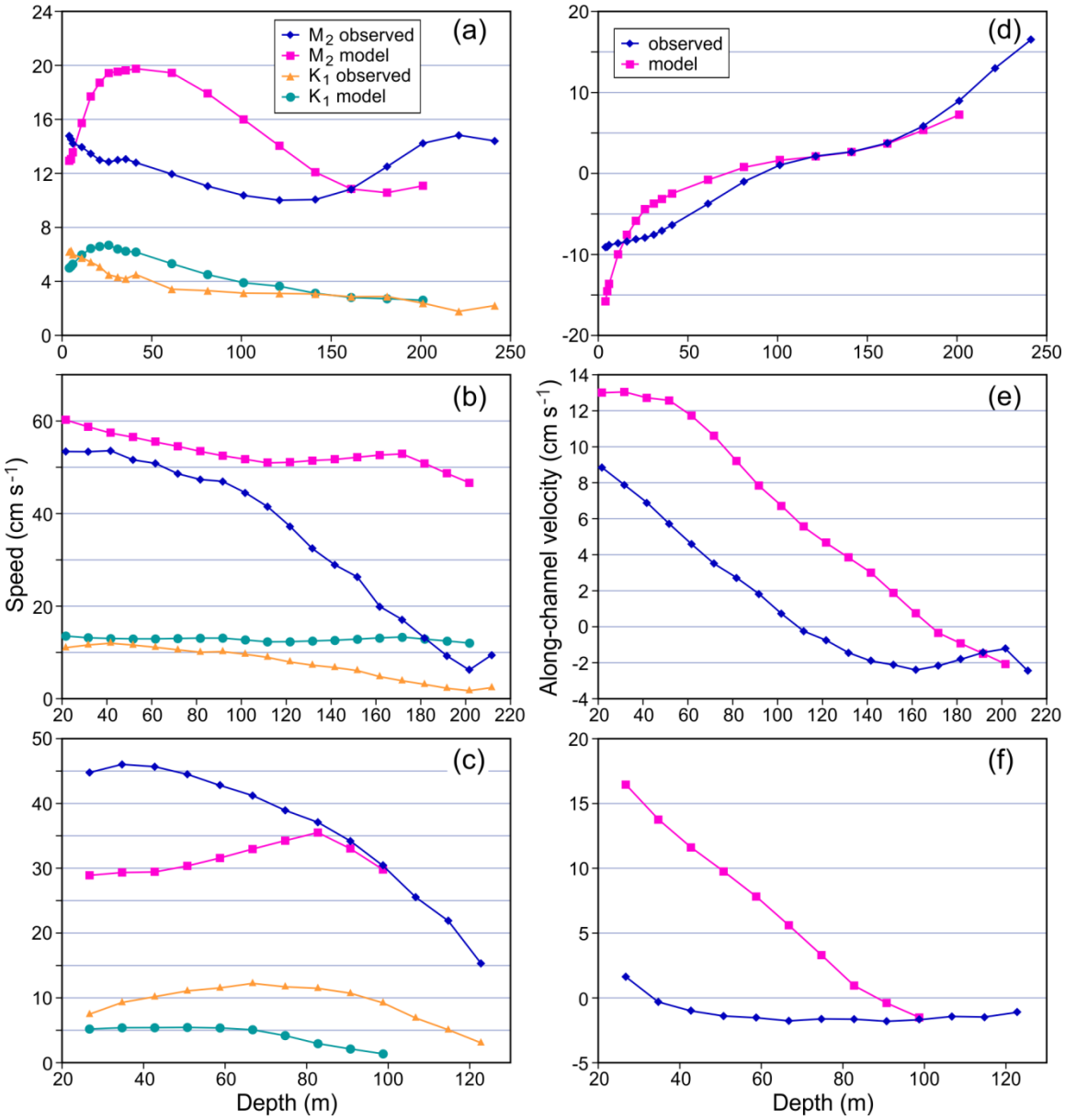

Figure 10. Modelled and observed vertical profiles of M2 and K1 tidal speed (semi-major axis) and mean along-channel current at the current meter moorings a) Nodales Channel (NC), b) Discovery Passage (DP), c) Cape Mudge (CM). For CM, "along-channel" was chosen as 160° counter-clockwise from east, the angle of inclination of the M2 major semi-axis. See Figure 6 for the location of these moorings. d), e), and f) are modelled and observed mean current profiles at the same three locations.

As a sample evaluation of the Discovery circulation model hindcast (with the coarser grid) for April 2010, Figure 10 (a, b, and c) compares model and observed vertical profiles of the M_2 and

K_1 tidal current amplitude, and the mean (April 4-28) current at the three mooring locations shown in Figure 6. As all tidal ellipses have very small semi-minor axes and there is close agreement between the model and observed angles of inclination, the flows are essentially rectilinear and our comparison can be restricted to amplitude (maximum speed). Generally, there is reasonable agreement between the modelled and observed K_1 amplitudes near the surface, but less so deeper in the water column. While the M_2 model surface speeds are also reasonably accurate at Discovery Passage, compared to observations they are too large at Nodales Channel, too small at Cape Mudge, and in general none of the three profiles capture the observed baroclinicity very well.

While the surface mean flows at Nodales Channel (Figure 10 d) are too large and those in the remainder of the southwestward, top-layer, estuarine flow are too small, values below 100 m are quite accurate. The thickness of the surface model estuarine layer (the flow direction change at 0) is seen to be about 70 m for the model and 90 m for the observed data. At Discovery Passage, the model flows are too strong virtually all the way down the water column and have much too weak and thin a bottom return flow. Finally, the model mean flow profiles at Cape Mudge show very little agreement with the observations. This mooring is south of Discovery Passage and its flow directions are not restricted by a relatively narrow channel. Whereas the observed mean flow directions range from northward at 26 m depth to southeastward at 122 m, the model mean flows are westward to northwestward over the entire water column. This disagreement is puzzling as the angles of inclination for the model and observed M_2 current ellipses agree very well, both being consistently in the range of 154° to 170° counter clockwise from east.

In this case, average D values (equation 1.4) for the M_2 and K_1 tidal constituents at eight tide gauge locations were 3.8 cm and 2.5 cm, corresponding to approximate errors of 4.1% and 3.2%, respectively. However, as described in more detail in Foreman et al. (2012), the primary deficiency with the Discovery circulation model simulations was the poorer representation of model currents deeper in the water column than at the surface. As both sea lice and IHN viruses originating from fish farms not only start at, but generally remain close to the surface where the model current accuracy is better, the subsequent dispersion calculation results for pathogens should also reflect that better accuracy. Nevertheless, the deeper inaccuracies warrant further investigation and could arise for a variety of reasons, foremost of which are probably mixing and the resolution of the grid and bathymetry. Clearly, this is a very complicated region in terms of coastal irregularities, bathymetry, and strong gradients in the flow regimes. A higher resolution grid that does a better job of capturing the details of these features has been constructed and the foregoing simulations will soon be repeated. Higher spatial resolution, particularly in regions with large depth gradients, will also reduce inaccuracies arising from the bathymetric smoothing that is needed to avoid hydrostatic inconsistency (Haney 1991), spurious (model artifact) flows, and too much mixing. The fact that all post-smoothing depths in the present simulations were greater than 5 m would certainly affect bottom frictional drag and contribute to current inaccuracies.

3. THE PASSIVE PARTICLE TRACKING MODEL

3.1. GENERAL OVERVIEW

In order to simulate the trajectories or dispersion of particles within our ocean model domain, an offline Lagrangian particle tracking model is used. It inputs 3D velocity, temperature, salinity and perhaps mixing fields computed and saved at regular intervals by FVCOM and uses them to disperse “particles” that are released at specific times and locations. The particle tracking module solves the following nonlinear system of ordinary differential equations (ODE)

$$\frac{d\vec{x}}{dt} = \vec{v}(\vec{x}(t), t) \tag{3.1}$$

where $\vec{x}$ is the 3D particle position at a time t, $d\vec{x}/dt$ is the rate of change of the particle position in time and $\vec{v}(\vec{x}, t)$ is the 3D velocity field computed by FVCOM. The ODE can be solved by a variety of methods but the one adopted here is the commonly-used explicit Runge-Kutta multi-step method. It is fourth-order accurate and for our purposes, that should mean it solves equation (3.1) very accurately. (See chapter 13 in Chen et al. (2011) for further details.) In some cases it may be desirable to also include a random walk-type process in the 3-D Lagrangian tracking code to simulate subgrid-scale turbulent (and other – e.g., due to missing tidal constituents) variability that has not been captured in the FVCOM velocity fields. This has been done for some of our passive particle tracking simulations (e.g. Stucchi et al. 2011) and those of Page et al. (2013), but care needs to be taken so that the random component is realistic. An issue that arises with particle tracking near coastlines is the procedure to follow when hitting a land or bottom boundary. After some trial-and-error testing we settled on a procedure which first determines if a particle will cross a land or bottom boundary in the next time step. If it were to do so, then the particle remains at the old location until at some future time, the velocity (and random walk) field is such that it moves the particle away and does not hit a boundary. In essence, this means that particles can become temporarily grounded but will float away when the velocity field allows that to happen.

Though the Runge-Kutta ODE solver has high accuracy, there are inaccuracies and uncertainties associated with our particle tracking. Of course, particle trajectories can only be computed for times and regions which have hydrodynamic output and their accuracy will be limited by the accuracy of the stored FVCOM velocities, and the particular random walk component. Of a more subtle nature, however, is the choice of frequency at which the FVCOM output has been stored. This is an issue because the Runge-Kutta solver takes much smaller time steps to compute the trajectories and for those times for which there are not FVCOM values, it does a simple linear interpolation between stored values bracketing the desired time. So if the velocities have non-negligible energy at periods shorter than the storage intervals, there will be inaccuracies in the trajectories. To date, almost all FVCOM storages have been hourly as that is usually sufficient to conduct a harmonic analysis that resolves the major tidal constituents. However, some experiments have been conducted to determine if that sampling interval is sufficient.

Figure 11 shows the average position and (x,y) directional standard deviations for a cluster of particles that were released simultaneously within a rectangular region in Queen Charlotte Strait and tracked for 2 days. The FVCOM simulation was for March 2009 and velocities were stored every 5 minutes so that subsamples could be taken at 5, 10, 15, 20, 30, and 60 minutes. No random walk was included in the simulations. As we would hope, the averages and standard deviations are seen to converge as the sampling time becomes smaller. The 15 minute sampling results are sufficiently close to those for 5 and 10 minutes that at least in this case, we conclude that should be an adequate interval for FVCOM storage. However, it is clear that the 1 hour values are sufficiently far away from those for the smaller intervals, that they are not adequate. As this result can be expected to be location and time dependent, it is not prudent to say that 15 minute sampling would always be adequate. Rather, before carrying-out a series of particle production runs for a particular model application, it would be wise to conduct a few experiments like those just described to determine an appropriate storage choice.

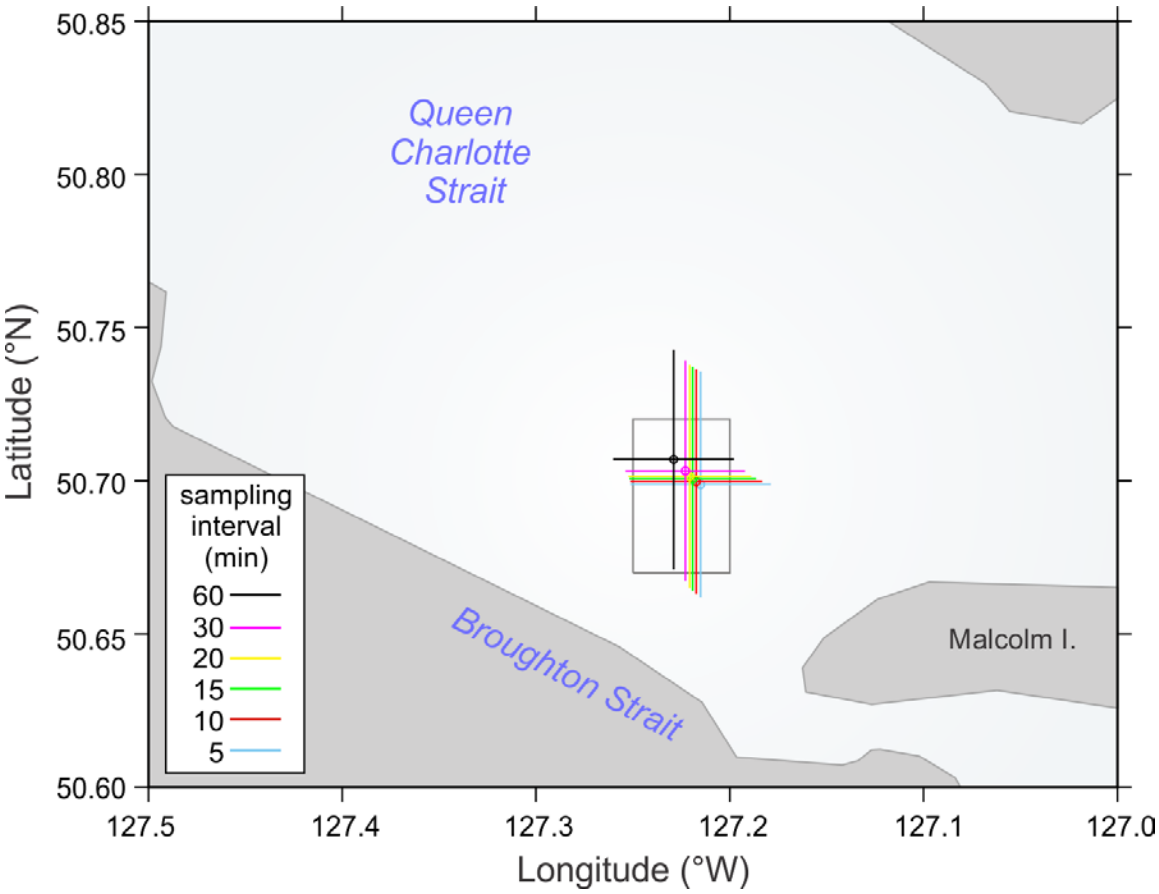

Figure 11. Average positions (coloured crossings) and (x,y) standard deviations (extent of crossing lines) for a cluster of particles that were released simultaneously and randomly over a rectangular region in Queen Charlotte Strait and tracked for 2 days.

3.2. BROUGHTON AND SOUTHWEST NEW BRUNSWICK EVALUATIONS AND APPLICATION TO BOTH THE BROUGHTON AND DISCOVERY REGIONS

GPS (Global Positioning System) drifter studies were carried out in the Broughton Archipelago in May, June and September 2006; March 2007; and March 2008. Though FVCOM simulations for 2006 and 2007 have not been run (as the weather stations were not yet installed, providing accurate atmospheric forcing would be difficult), they have been done for March 2008 (e.g., Foreman et al. 2009) and this means that passive particle tracking evaluations can be carried out.

The GPS tracked drifters were deployed on March 26 (Knight Inlet) at the locations crossing Knight Inlet north of Protection Point as shown in Figures 12; all were designed to drift with the surface currents using a drogue extending from the sea surface to a depth of one meter. The drifters were tracked for a maximum of thirty-three hours, however only two remained free floating for the entire length of time; the remaining four grounded along the shoreline after 7, 15, 19, and 17 hours of being released.

To compare the observed drifter trajectories with modelled trajectories the particle tracking model simulated the release of one thousand particles randomly distributed over the top 1 m of the water column at each of the six drifter starting points; each particle position was updated every 30 minutes. Given the FVCOM model output has a time resolution of one hour the timing of the particle releases was within one hour of the time of the drifter releases The FVCOM

horizontal velocities were taken from a simulation analogous to that described in Foreman et al. (2009), but with the higher resolution grid and heat flux forcing. The vertical velocities from FVCOM were not applied to the particle movement as the actual drifters remained at their initial depth in the top 1 m and could not respond to vertical forcing.

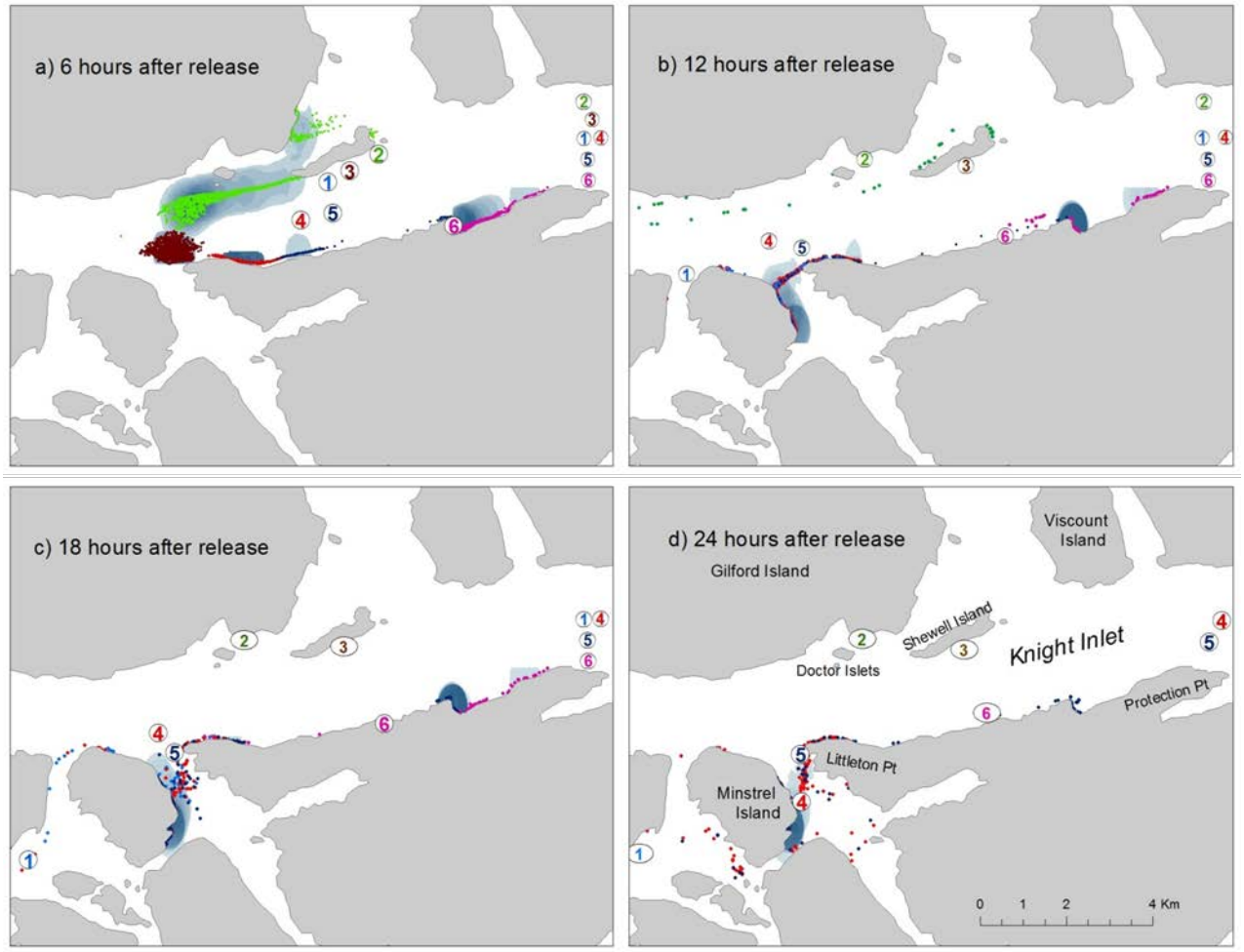

Figure 12, A comparison of observed surface drifter locations and the positions of particles simulated using a passive particle trajectory model and the output of FVCOM. The six drifters are identified by number and colour and the simulated particles are coloured corresponding to the drifter's position where the particles were released north of Protection Point.

Figure 12 compares the observed positions of six surface drifters with the simulated particle dispersion at six hour intervals. Each drifter is identified by number (one through six) and each panel shows the location of the start point and the location after the time period (6, 12, 18 and 24 hours) for each drifter that had not grounded. Figure 12 also shows the positions of particles modelled using the particle trajectory model and colour coded by the starting location of each of the six drifters. The blue coloured clouds in each panel of Figure 12 represent clusters of simulated particle positions, with the deeper blue colours associated with a greater point density of the particles.

The interpretation of panel a) in Figure 12 shows five of six drifters having moved 4 – 7 km to the west of their starting positions, similar in the direction, but with less distance than their corresponding model particles. This initial inconsistency in distance travelled may be explained by the output from FVCOM being applied with a one hour time step whereas the GPS drifters

are responding to forcing with positional updates every two minutes. While five of the drifters stayed mid-channel the most southerly drifter (coloured magenta) moved to the south coast of Knight Inlet, as did all of the simulated particles released at that point.

After 7 hours of travel drifter 3 had grounded on Shewell Island and therefore in panel b there are no 12 hour particle positions (brown colour) representing drifter 3. Of the other five drifters most are spread out along the south shore of Knight Inlet, with the exception of drifter 2 which is in the vicinity of Doctor Islets on the north shore. The green particles that correspond to drifter 2 are also positioned along the northern shore of Knight Inlet.

After 18 hours (panel c) it is evident that there are two areas where the particles are higher in density; along the eastern shore of Minstrel Island, and to the west of Protection Point on the south shore of Knight Inlet. This is supported by the positions of drifters 4, 5 and 6. Drifter 2 has grounded by Doctor Islets, and drifter 1 (light blue) has travelled the furthest, although still within the range of light blue particles.

Panel d represents drifter and particle positions 24 hours after release. By this time four of six drifters have grounded reflecting a large footprint (see the final locations of drifters 1, 2, 3, and 6). Those still free-floating are located within this footprint, and in the region of the densest cloud of particle positions.

The simulated movements of 6000 particles compared to the tracks of six drifters revealed that FVCOM model output at a one hour time step will initially (up to six hours) create inconsistency between the modelled and observed positions. Comparisons at later times show good agreement between the drifter positions and the cloud of particles. It is apparent that both the simulated particles and the drifters followed paths away from the mid-channel and towards the shorelines. Whereas the model allowed particles to continue moving after shoreline contact had occurred, the actual drifters stopped moving once they encountered the shoreline. Adjusting the trajectory model parameters governing shoreline behaviour may improve the agreement between particles and drifters.

An example of information provided by trajectory modelling that is often unobtainable by carrying out drifter studies is shown in Figure 13. This figure relates to Figure 12 b) showing the positions of particles 12 hours after being released at the starting point of drifter 2. The drifter track shows a path westward along Knight Inlet to its eventual grounding point near Doctor Islets. The trajectory model includes this path as similar to one of those taken by a few of the 1000 particles released. The model also shows that a significant majority of numerical drifters continue to move along the south shore of Gilford Island and accumulate in the area of Turnour and Village Islands. In this case the position of the drifter falls within the footprint of numerical drifters, but the model shows a likelihood of surface transport greater than that experienced by the drifter.

As the numerical drifters do not become permanently grounded, rather they hold their position until the currents change and allow them to move away from the shore, their behaviour cannot be expected to be the same as the actual drifters. This may be why the numerical drifters seem to proceed further along the shorelines than their real counterparts. (Of course, inaccurate velocities provided by the FVCOM simulation may also explain many of the trajectory differences.) Nonetheless, we feel there is a reasonable agreement between the actual and numerical drifter tracks in the sense that the real drifters travelled within the dispersion plume determined by numerical drifters.

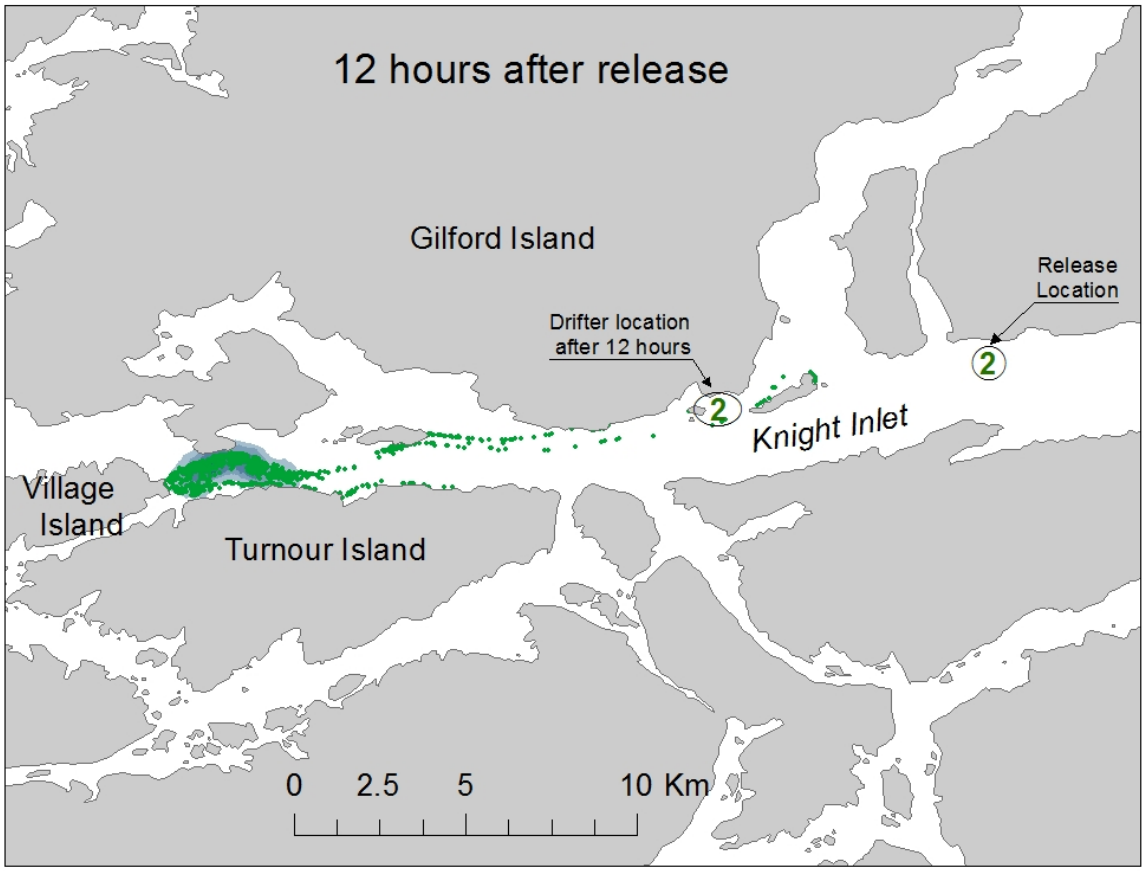

Figure 13. A comparison of the positions of 1000 numerical drifters and drifter 2, 12 hours after being released.

Page et al. (2013) present a much more extensive evaluation of their FVCOM circulation and particle tracking application in southwest New Brunswick (SWNB). In this location, sea lice have become resistant to the in-feed treatment that is still effective in BC and the aquaculture industry has resorted to therapeutant bath treatments that have the potential to impact other biota once they leave the fish farm net pens. In addition to its offline and online particle tracking capabilities, FVCOM also has an online dye concentration module that solves advection diffusion equations similar to those for salinity and temperature (eq. 2.5 and 2.6). While one might think this dye module would be the natural choice for modelling the evolution of therapeutant concentrations, numerical experiments conducted by Page et al. (2013) revealed horizontal dispersion rates that were too large compared to the dye observations. Experiments with a finer grid demonstrated that this overestimation was due to having too large a grid cell size and as experiments using the particle tracking approach showed that its dispersion was independent of grid size, it was chosen over the dye module. However, an offline dye module that the FVCOM developers claim should be more accurate is now available (C. Chen, personal communication), so efforts are planned to conduct further experiments and establish how well it performs.

The SWNB circulation model was calibrated and evaluated against an extensive array of tide gauge and current meter data, including several acoustic Doppler current profilers (ADCPs) that

were placed near the cages so that the effects of the cage structures on the flow could be assessed. Drifters were also launched and tracked and a fluorescent dye was mixed with the bath treatments at three locations so that it would be visible and easily tracked once it left the cage. Discrepancies between modelled particle tracks and the observed dye dispersion were found and typically traced back to inaccuracies in FVCOM's representation of the dominant tidal constituent, M_2. In particular, Page et al. (2013) demonstrated that even when the model and observed sea surface elevation amplitudes and phases and the tidal current ellipses amplitudes had good agreement, the tidal current phases could still be poorly predicted by the model (in one case they differed by 1.25 hours) and this had important implications in matching the modelled dye release with the experimental field data.

The Page et al. (2013) particle tracking experiments also determined that the horizontal and vertical diffusion coefficient values best matching the observed dye dispersion were 0.1 $m^2 s^{-1}$ and zero, respectively. Several comparisons were made between particle tracking model predictions, dye perimeter observations and actual drifter tracks. Though in some cases the model dispersion compared quite well with the observations, in others it did not. Discrepancies were attributed to several factors, the most important of which were missing features in the FVCOM velocities provided to the particle tracking code. As the model was forced with only the barotropic tides, the inclusion of winds, heat flux, and freshwater discharges should improve FVCOM's accuracy. However, subsequent experiments indicated that including a surface drag associated with the cage structures (Wu et al. 2014) was the most important missing feature.

A series of passive particle tracking simulations have been carried out in the Discovery Islands region using velocities computed with the coarse grid circulation model. One particle was released per hour at each of thirty-two farms and tracked for 10 days, a period which is a reasonable representation of the lifetimes of both viruses and pre-infective sea lice. The particles were released randomly at depths between 5 and 10 m (the mid-depth of a typical net pen) over a time period from April 1 to October 22, 2010.

Figure 14 shows the April dispersion clouds arising from the release of particles at all farms after 2.5, 5.0, 7.5, and 10 days. Notice that despite a predominant surface estuarine flow that should, on average, transport particles to the north and northwest, some have moved to the southeast into the Strait of Georgia. Also notice that particles are building up along the western boundary in Johnstone Strait. The fact that they are accumulating and not cleanly escaping is an artifact of the boundary conditions in the particle tracking model and is not realistic. (At present, open ocean boundaries are treated the same as land boundaries, a feature which is being addressed in recent model developments). This accumulation suggests that particles can move out of the Discovery region into the Broughton region. To better understand exactly where they go from there, and in particular whether they could be transported near a Broughton farm, particles were seeded near the southeast Johnstone Strait boundary in the Broughton model. Those results will be discussed later (see Figure17).

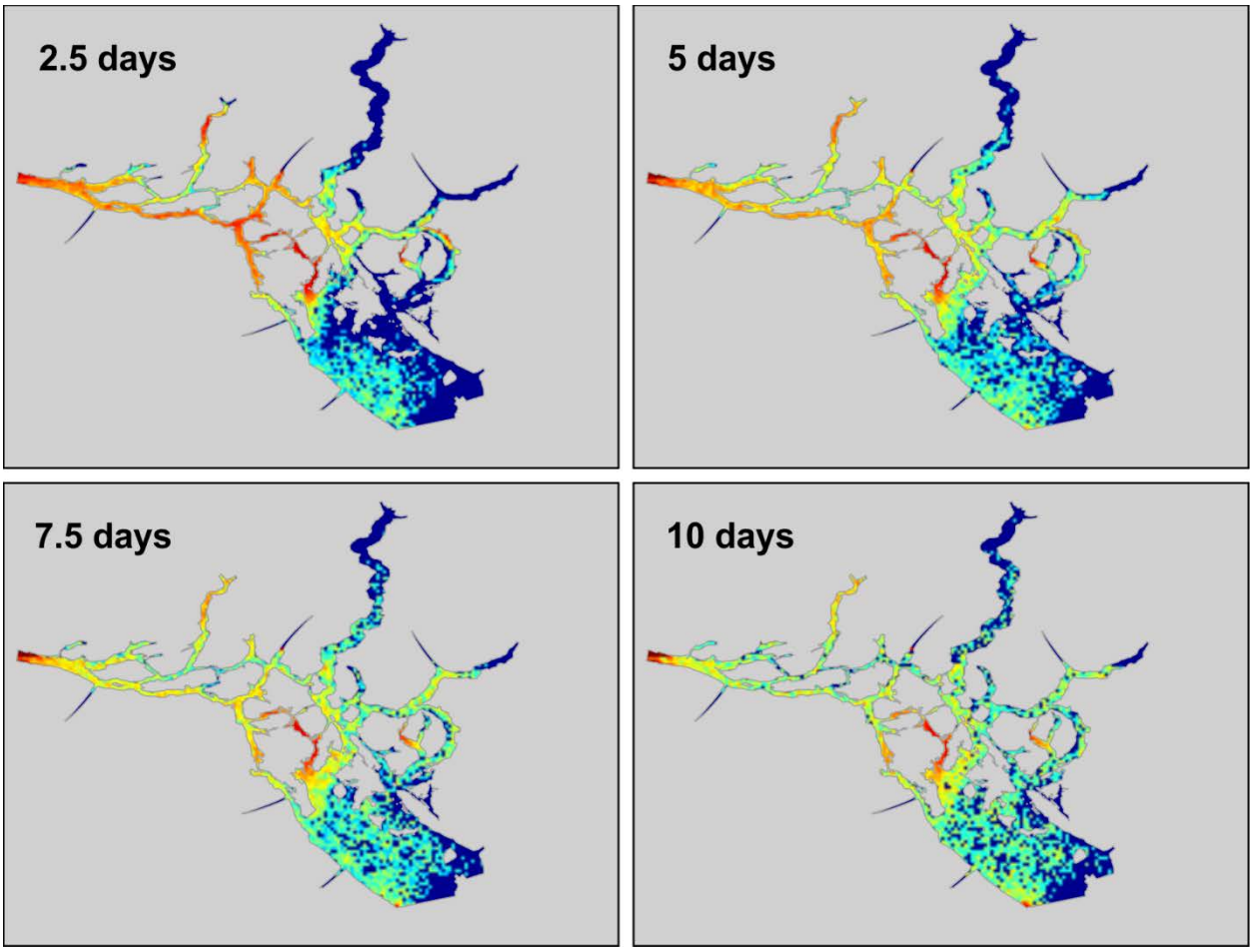

Figure 14. Dispersion clouds after 2.5, 5, 7.5, and 10 days arising from hourly particle releases over the month of April, 2010 at 32 farms within the Discovery Islands region. Red (turquoise) colours denote higher (lower) concentrations.

Another way of determining major dispersion routes and accumulation areas is to compute the number of particles that cross transects lying across significant channels. Figure 15 shows the Discovery Islands model domain with 13 transects listed in the caption.

As fluctuating tides may cause a single particle to cross the same transect several times, we only count particles that have crossed transects an odd number of times (i.e. those that ultimately end up on the opposite side of the transect from which they started).

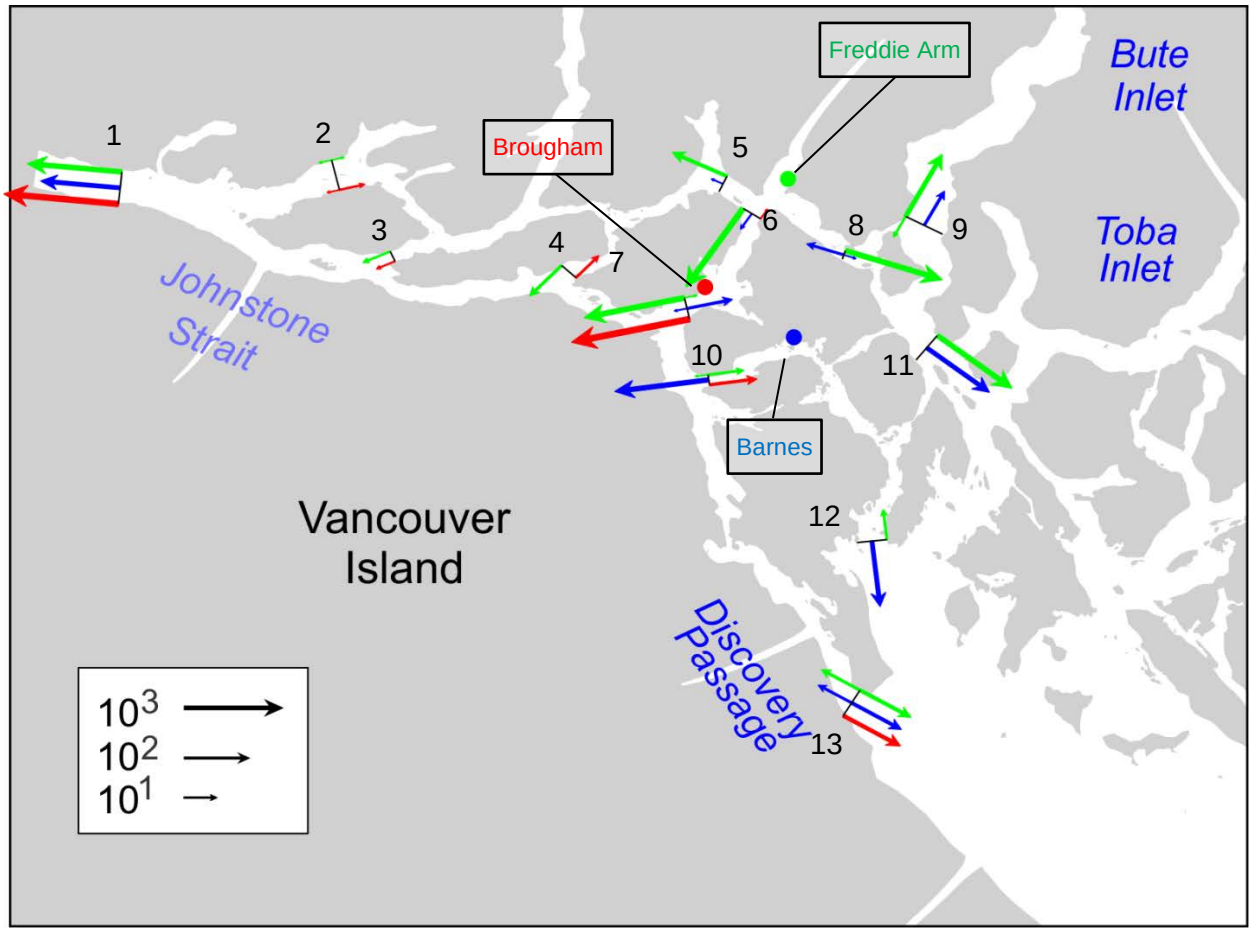

Figure 15. Particle fluxes from the April 2010 simulation originating from net pens at the Freddie Arm (green), Brougham (red), and Barnes (blue) farms and crossing key channel transects (black): 1 Central Johnstone Strait, 2 Central Sunderland Channel, 3 West Chancellor Channel, 4 West Mayne Passage, 5 Central Cordero Channel, 6 North Nodales Channel, 7 South Nodales Channel, 8 South Cordero Channel, 9 South Bute Inlet, 10 West Okisollo Channel, 11 Calm Channel, 12 Hoskyn Channel, 13 South Discovery Passage. Note the logarithmic scaling of the arrows.

Figure 15 shows the results of simulations for passive particles released from the Freddie Arm (green dot), Brougham (red dot), and Barnes (blue dot) farms sites in April 2010. The colour and length of the vectors at each transect reveal the origin and the number of particles that crossed the transect. Note that several transects have vectors going in both directions. This means that some particles have taken an alternative route into or out of a channel. For example, the green vector entering Discovery Passage from the Strait of Georgia would denote Freddie Arm particles that have entered the Strait of Georgia via either the Hoskyn or Calm Channel routes.

It is seen that approximately 48% of the Freddie Arm particles enter Nodales Strait, approximately 48% go southward in Cordero Channel and approximately 4% go northward in Cordero Channel. Of those entering Nodales, almost all (approx. 95%) pass completely through the strait and enter Discovery Passage within 10 days. Of those, roughly 95% go northward and cross the Johnstone Strait transect while 5% go southward and cross into the Strait of Georgia.

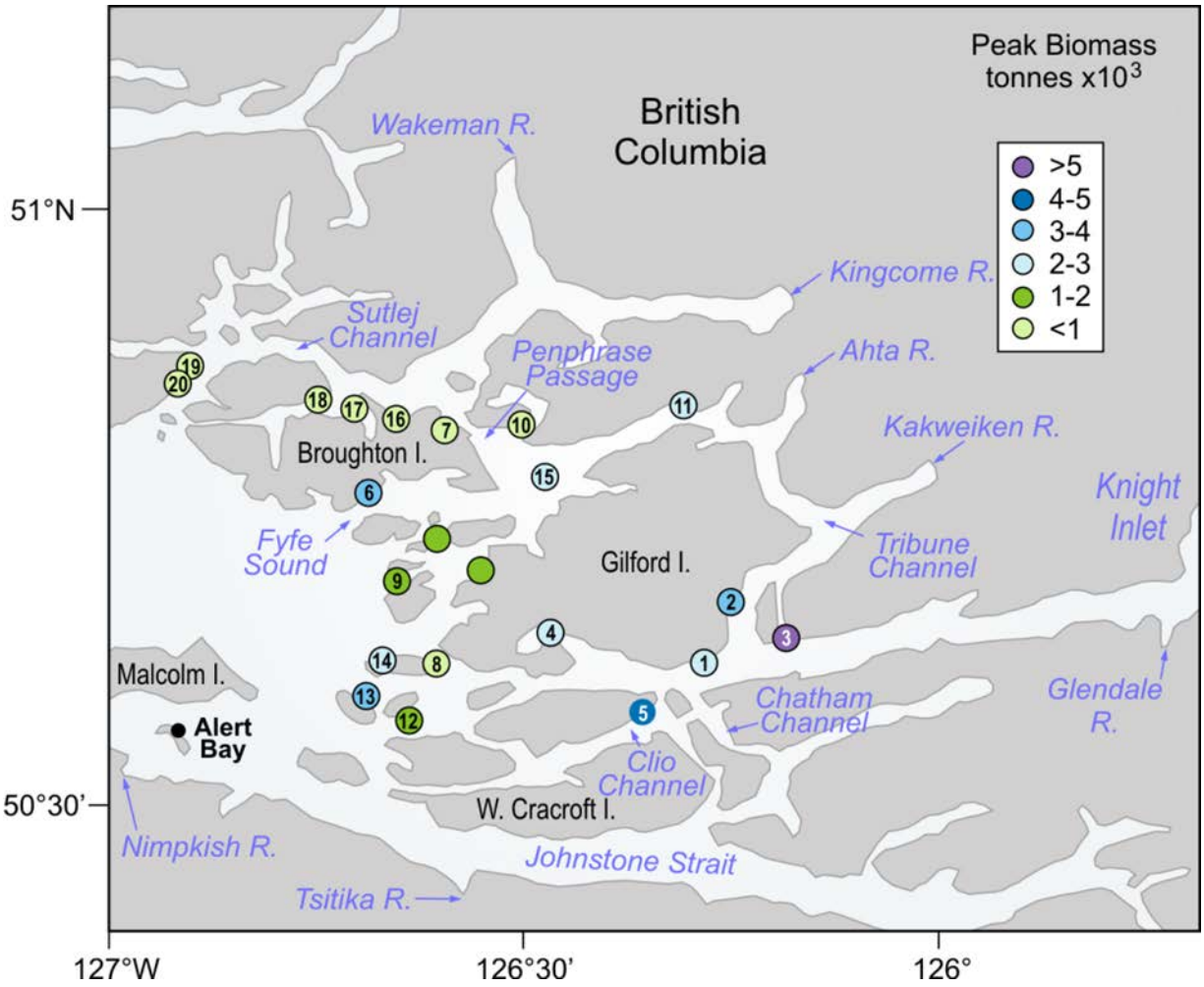

Figure 16. Broughton Archipelago farms where passive particle releases were simulated. Farm identification numbers correspond to those used in Table 2. Circle colour denotes the farm's peak biomass (tonnes x10^3) set by the 2013 licence.

The fine-resolution Broughton Archipelago grid was used to simulate the release of passive particles from twenty farms within the archipelago (Figure 16). The FVCOM hydrodynamic modelling and subsequent particle tracking simulations were carried out for March to July 2009 (as that year had a minimal number of missing atmospheric data). Fifty particles were released each hour at points randomly distributed within a three-dimensional rectangle (100 m by 100 m by 10 m) defining a farm and tracked for a period of eleven days. The results of passive particle tracking are based on simulations representing 27 days in March 2009. A connectivity table was computed to characterise transfers between farms; a particle was deemed to have arrived at a farm if, at any time, its trajectory lay within the rectangular area that defined the capture farm. As this included the release farm, the largest number of connections was always with the farm of origin. Although a more thorough analysis will be performed by Erin Rees (University of Prince Edward Island), Table 2 shows preliminary connectivity results for releases over March 2009.

Table 2. Passive particle trajectory modelling estimates of the connectivity among the twenty farms shown in Figure 16. Higher (lower) connectivity is denoted by redder (bluer) colours. White cells denote zero connectivity.

	release farm																			
capture farm	1	2	3	4	5	6	7	8	9	10	11	12	13	14	15	16	17	18	19	20
1	29867	4078	2372	135	339	25	85	28	3	14	118	1	3	13	25	1	4	-	-	-
2	282	32400	3032	4	47	82	205	5	9	96	442	-	3	3	180	11	11	2	-	-
3	236	833	22134	20	80	-	3	3	-	1	14	1	-	1	1	-	-	-	-	-
4	1241	311	363	21113	64	-	1	20	-	-	-	5	4	4	-		-	-	-	-
5	1030	369	448	620	21784	1	2	281	51	-	2	121	61	148	7	1	-	-	-	-
6	29	14	16	41	14	32400	390	294	339	463	665	158	255	322	1445	41	33	6	10	20
7	-	-	-	-	-	8	32400	-	-	517	225	-	-		265	801	1078	521	86	31
8	1887	640	528	3241	954	69	81	32400	3576	103	322	3284	2595	9972	795	4	1		1	1
9	50	9	19	85	25	111	120	429	32400	137	454	231	323	548	968	10	5			
10	-	2	2	-	-	13	585	2	4	19473	471	-	1	1	322	86	74	22	5	6
11	4	218	190	2	-	346	982	40	85	616	16899	13	34	53	877	87	98	28	9	13
12	291	64	69	416	814	3	1	943	229	1	6	15775	1383	517	38	-	-	-	-	-
13	528	147	181	808	393	5	5	2113	850	12	32	4770	15449	1437	88	1	-	-	3	7
14	1403	464	380	2337	681	39	48	12477	3068	71	227	2755	2365	32400	565	5	1	-	2	2
15	4	58	61	14	5	883	1865	156	213	2165	5917	85	127	190	32400	211	221	53	31	34
16	-	-	-	-	-	96	136	4	11	23	16	1	12	10	20	11945	10017	5482	2058	908
17	-	-	-	1	-	36	9	4	3	1	-	-	6	6	2	2014	12491	4827	658	381
18	-	-	-	-	-	17	4	1	-	-	-	-	3	7	-	1164	1641	19349	289	169
19	4	1	3	9	1	805	36	112	164	16	28	90	140	178	69	1850	1016	656	32400	10229
20	21	-	4	11	2	1125	31	160	195	19	31	150	197	236	100	1274	689	459	14866	32400

In Table 2 the top axis identifies the farms at which particles were released, and the left axis those farms where the particles were captured. The diagonal signifies self-impact, and while for many farms the number therein equals the total number of particles released, for others (e.g. farm 16) strong currents in the vicinity of the farm advect many particles more than 100 m from their release point within the first hour. Table 2 can be interpreted as a heat map where 'hotter' colours symbolise a greater impact on the farm site. Symmetry about the diagonal (e.g. farms 14 and 8) indicates a mutual exchange of particles while asymmetry can largely be explained by the average background (surface estuarine) flow fields, as shown in Figure 5a of Foreman et al. (2009). For example, farms 1 and 3 show a clear bias with particles from farm 3 ten times more likely to reach farm 1 than vice versa.

Following the Discovery passive particle release experiments that showed an accumulation of particles along the Johnstone Strait boundary (Figure 14), the trajectory model was used to simulate the release of particles at the Johnstone Strait boundary of the Broughton model domain. Specifically, particles were released hourly over a twenty day period at three sites across the Johnstone Strait boundary and tracked for ten days (Figure 17). Note that whereas the Discovery releases were for April 2010, there was no coincident wind data for the Broughton Archipelago at that time so instead we took the FVCOM velocity fields for March 2009. As the objective of this experiment is to determine if there is a potential for disease and/or parasite transfer from Discovery farms to Broughton farms, not to simulate dispersion for a specific time period, this timing mismatch should not make much difference. Figure 17 suggests that a transfer to Broughton farms, especially those nearest the seaward part of the archipelago, is possible. However we have yet to compute the total transit times for these particles (to be consistent with the Discovery simulations, they should be eliminated after a total of ten days in the water) or account for the effects of salinity, temperature, and UV radiation on biological (versus passive) particles. Further analysis is needed before more definitive conclusions can be made.

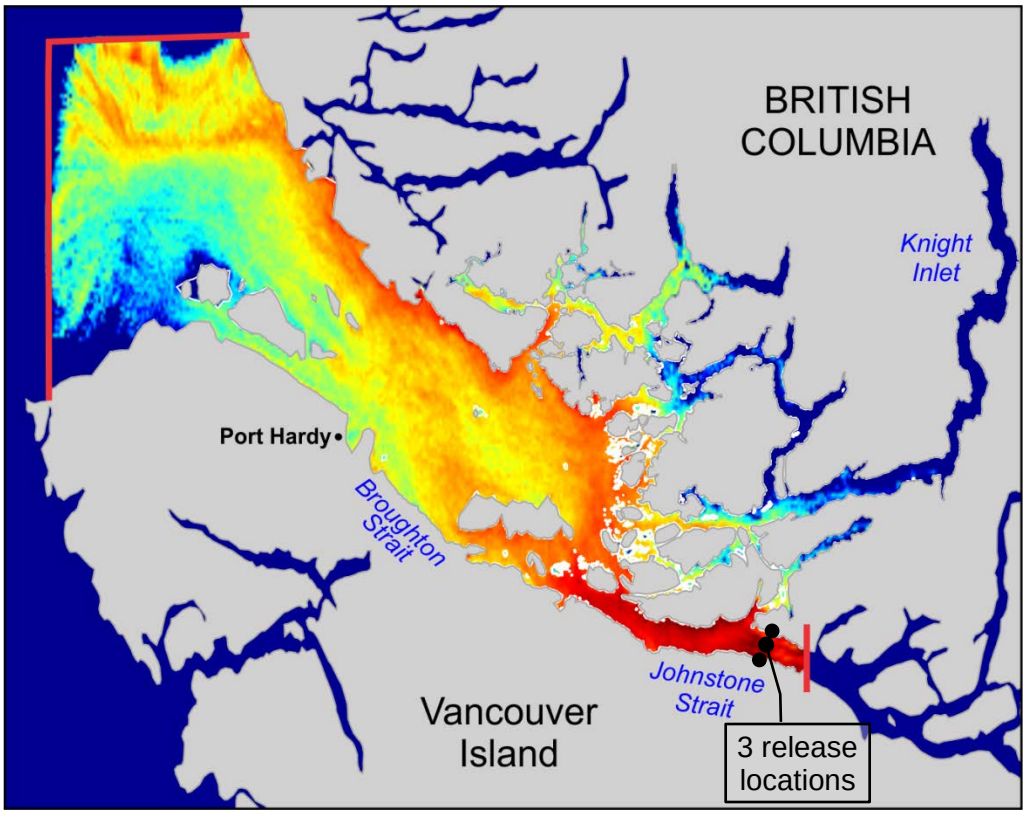

Figure 17. Proportion of particles released near Johnstone Strait model boundary reaching locations within the Broughton model domain at some time during their ten day excursions. Deep red denotes near 100% likelihood and royal blue near 0%.

4. THE NON-PASSIVE (BIOLOGICAL) PARTICLE TRACKING MODELS

4.1. OVERVIEW AND REQUIREMENTS FOR APPLICATION

The biological particle tracking model is similar to the previously-described passive model except that the particles i) can be assigned characteristics that are dependent on their ambient surroundings, and ii) may no longer be passively floating with the background currents. That is, they can be assigned behaviour (e.g., swimming or sinking capabilities) and/or given biological or chemical attributes that, for example, simulate life stage progression and mortality dependencies or a degradation into different substances. As such, the particle tracking model can provide an indication of how organisms or pollutants originating on aquaculture sites disperse throughout a region.

The Broughton sea lice (*Lepeophtheirus salmonis*) model (Stucchi et al. 2011) therefore not only requires time-varying 3D velocity, temperature, salinity, and mixing values from the associated hydrodynamic model, but also an understanding of the biology and environmental factors affecting sea louse early life stages. The model only simulates the production of sea lice eggs from salmon farms and the development and mortality of the planktonic larval stages (nauplii I, nauplii II, and copepodid). It does not attempt to represent the life history after copepodids find a host and progress through the chalimus, pre-adult and adult phases. Several biological parameters are required by the sea lice model and though laboratory studies (e.g., Johnson and Albright (1991), Heuch et al. (2000), Stien et al. (2005), Bricknell et al. (2006), Hayward et al. (2011)) do provide some guidance on the required values or relationships,

considerable uncertainty remains on both the specific values employed (as they are based on small statistical samples) and the applicability of relationships derived from laboratory studies to realistic oceanic conditions. As a consequence, there is also considerable uncertainty around the copepodid concentrations provided by our particle tracking model. Though it would be valuable to conduct sensitivity studies to estimate the magnitude of these uncertainties, this has yet to be done.

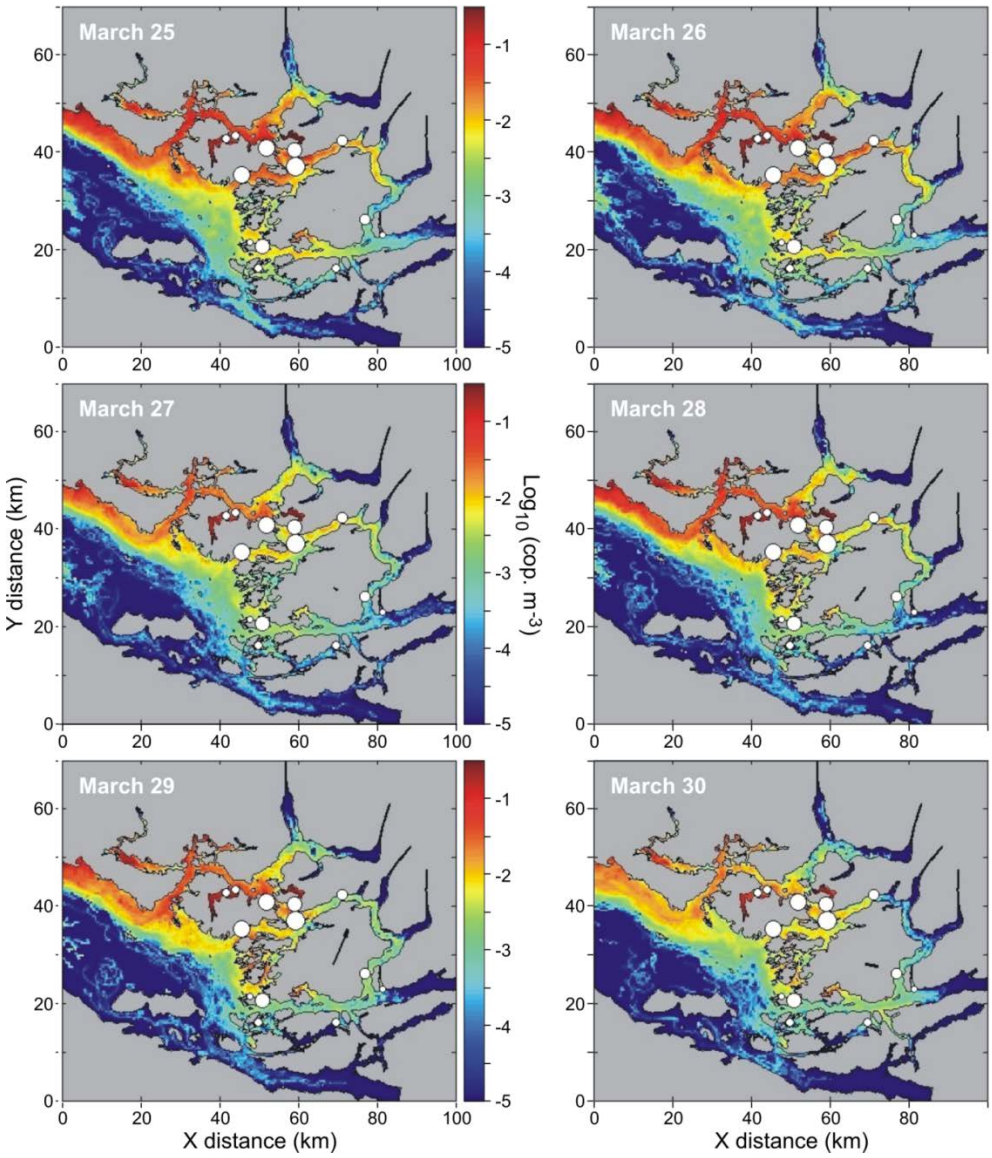

Figure 18. Daily average surface concentrations of passive (no diel migration) copepodids from March 25 to 30, 2008. Locations of the farms producing sea lice are shown by the white circles and the relative strength of farm sea lice source is represented by the diameter of each circle. Note the persistent higher concentrations along the northeast shore of Queen Charlotte Strait.

The total daily production rate of active nauplii from an operational salmon farm is given by the product of i) the rate of viable egg production by an adult female sea louse, ii) the average number of adult females per fish on a farm, and iii) the number of fish on a farm. The latter number is available from industry while the second number is estimated by regular (and DFO regulated) sampling carried out on each of the farms. The egg production rate is the product of

i) the average number of eggs in female egg strings (estimated from sampling), ii) the proportion of eggs that hatch and develop into actively swimming nauplii (a function of salinity based on the laboratory experiments of Johnson and Albright (1991)), and iii) the inverse of the minimum egg development period (a function of temperature based on the Stien et al. (2005) laboratory studies).

Once these parameters are obtained, the sea lice model then proceeds by releasing a prescribed number of particles (typically 50-100) from each of the active Broughton farms every hour for a prescribed length of time and tracking their dispersion for a fixed time period. Each particle represents a cohort of sea lice so that by the end of the tracking period, the model not only provides a history of the 3D trajectory of that cohort, but also an estimate of the percentage that survive to the copepodid life stage and that die in each of the egg, nauplii, or copepodid life stages. Larger release numbers allow a better estimate of overall dispersion patterns but require more computation time; hence the 50-100 compromise. The hourly release rate is another compromise between computation time and the need to capture changes to the tidal and wind-driven components of the currents. The actual particle tracking technique uses the same 4^{th} order Runge–Kutta algorithm that was previously described for passive particles and can include a random walk component. Diel vertical migration can also be included at the copepodid life stage, though studies carried out in the Broughton Archipelago with a 10 m vertical column suspended in the ocean showed that copepodids did not exhibit any depth preference during the day- or night-time (A. Lewis, personal communication). See Stucchi et al. (2011) for further details. Though the Broughton sea lice model has been applied to the Discovery Islands and tested with fictitious farm data, a realistic simulation has yet to be carried out.

The Discovery IHNv model is a relatively simple modification of the sea lice model that incorporates different biology. In this case, the relevant parameters or relationships are i) the viral shedding rate from an infected farm, ii) the viral survival rate in the marine environment, and iii) the minimum infective dose required to infect otherwise healthy fish. The necessary parameters were estimated by a series of laboratory experiments whose methodologies and results are described in Garver et al. (2013). The abundance of IHNv in seawater was found to be largely determined by sunlight (UV) penetration and the presence of natural biota (e.g., bacteria). As the circulation model does not estimate UV radiation, it had to be estimated from UV radiation measurements (A and B spectra) collected by an erythmal sensor at many of the Discovery weather stations. Additional laboratory measurements determined the UV decay rate as a function of depth from the water surface. Though this was done for water collected from the Strait of Georgia near the Pacific Biological Station (PBS), it will be highly dependent on particulate material in the water column and can be expected to vary in both space and time throughout the Discovery region. As there are no measurements to estimate these variations, this UV decay with depth may be a considerable source of uncertainty in our subsequent estimates of virus survival in the marine environment. Otherwise the particle tracking was very similar to that for the sea lice model. Again, released particles represented cohorts of IHNv and temporally and spatially dependent viral concentrations were computed to determine if neighbouring farms to those with disease outbreaks could also become infected via water-borne transmission.

4.2. RESULTS FROM, AND EVALUATION OF, THE BROUGHTON SEA LICE PARTICLE TRACKING MODEL

An extensive description of results from, and an evaluation of, the Broughton sea lice dispersion model using circulation model results from the March 13 to April 2, 2008 simulation is presented in Stucchi et al. (2011). The following is a brief summary.

Simulated particles were released at the locations of 14 active salmon farms with a rectangular box (100 m × 100 m × 10 m) representing the net cage structure of the farm. Within this box, 20 randomly located particles were released every hour for 11 consecutive days giving a total of 5,280 releases at each of the locations. The releases began on March 18, stopped on March 28, and each particle was tracked for 11 days. Though the tracking could have been continued, copepodids are believed to die if they cannot find a host within a specific time period. Though there are varying opinions about what that period should be, our nauplii generally reached the copepodid stage in 4-5 days and so an 11-day total tracking period allowed approximately one week for a copepodid to find a host. Each released particle represented a cohort of nauplii with the number of individuals in each cohort being determined by the daily egg production on individual farm sites. Time and spatially varying salinity fields from the model were used to determine egg viability and the daily release of active nauplii from each farm. Simulations were run with and without diel vertical migration swimming behaviour for the copepodids. Daily average concentrations or densities of the infective copepodid stage were calculated from March 25 to 30 and those for the surface layer (0 to 5 m depth) without diel migration are shown in Figure 18.

The highest computed concentrations are seen to be around one copepodid in 10 m^3 of water (0.1 m^{-3}), but most regions have much lower concentrations. The simulations with and without diel vertical migration generally did not differ significantly from each other. Both show a 5 to 10 km wide band of copepodids at relatively high concentrations hugging the northeast shore of Queen Charlotte Strait. In both simulations, concentrations in this band are comparable in magnitude and relatively high at ~0.1 copepodids per m^3 compared to most other areas in the model domain. Inside the study area, the passages surrounding Broughton Island (Fyfe Sound, Penphrase Passage, Sutlej Channel; see Figure 2) also show high (10^{-1} to 10^{-2} copepodids m^{-3}) concentrations in both simulations. Concentrations in and around the Tribune Channel–Knight Inlet junction range from nearly zero to ~10^{-3} copepodids m^{-3}. In Knight Inlet east of the junction with Tribune Channel, both simulations produce very low concentrations of copepodids (~10^{-5} m^{-3}). Temporal changes in the modelled concentrations are mainly due to wind effects. From March 25 to 28 winds in Knight Inlet were westward but switched to the east late on the 28th, with several strong easterly wind events occurring in the next few days. Higher concentrations of copepodids occurred in Knight Inlet near the junction with Tribune Channel and in the passages to the south on March 29 and 30 than earlier in the simulation period. The wind appears to have reversed the seaward surface flow and moved water with higher copepodid concentrations eastward in Knight Inlet, and southward into Clio and Chatham Channels (Figure 2). Current meter observations from the Knight Inlet mooring (and extension of those shown in Figure 7) confirmed the reversal in surface flow starting on March 29, 2008.

The copepodid concentrations shown in Figure 18 arise from eggs originating on fourteen farms. However, because the particle tracking output includes a complete history of positions arising from each release, it is relatively easy to separate these concentrations into contributions from individual farms and thus provide a time-dependent footprint for each farm. Figure 19 shows an example for March 26 and nine of the farms. In this particular case, the footprints are seen to be considerably larger for up-estuary farms such as Humphrey Rock and Watson Cove, suggesting that they pose a greater risk of dispersing sea lice to juvenile salmon and other farms, than downstream farms like Wicklow.

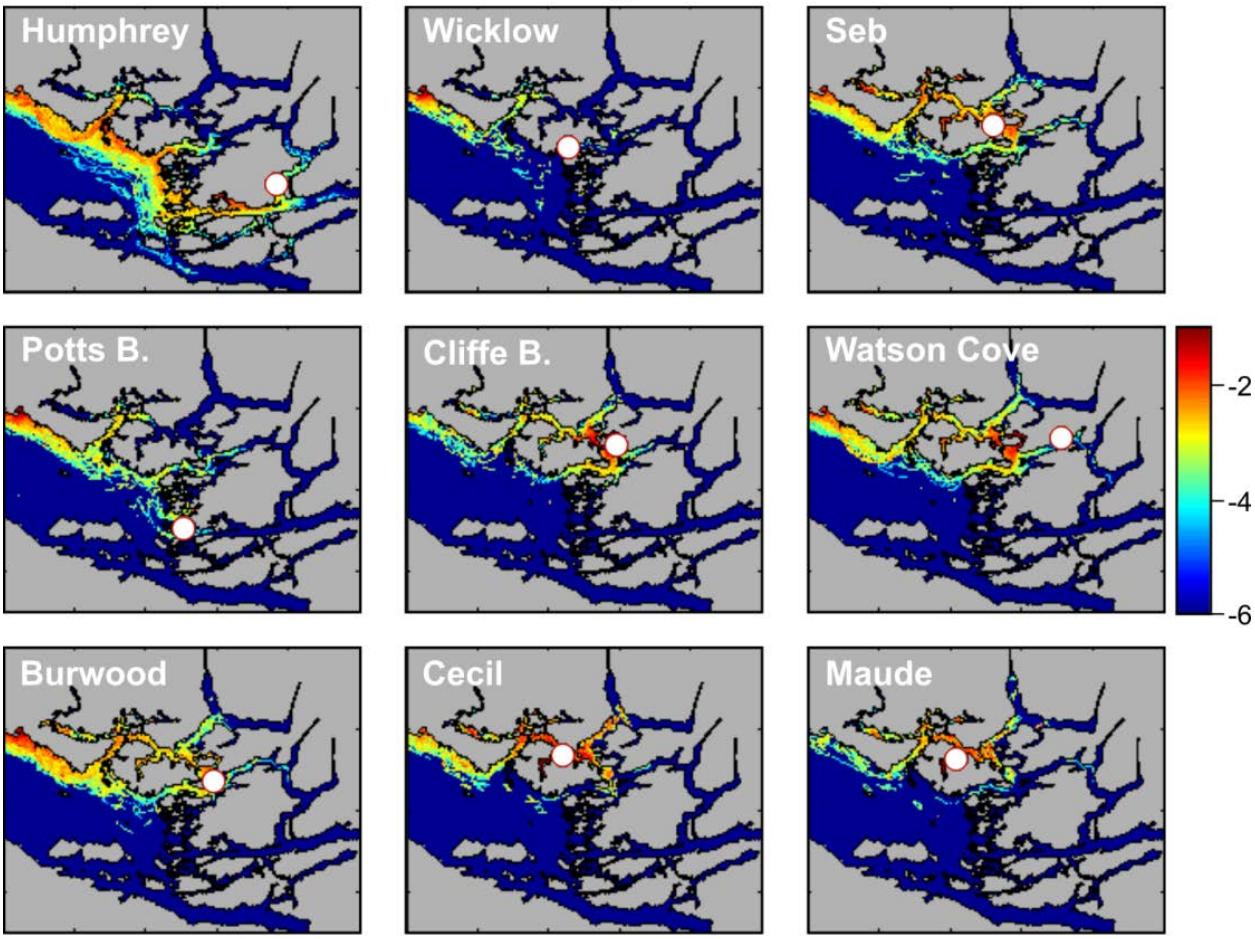

Figure 19. March 26 average surface concentrations (log_{10} sea lice m^{-3}) of passive (no diel migration) copepodids arising from the nine farms designated by the white circles.

There are two types of field observations that allow at least the possibility of evaluating these lice concentration estimates. The first are plankton net tows while the second are wild fish surveys. From March 25 to 29, 2008, 28 plankton net tows were carried out by Moira Galbraith at different locations in Knight Inlet and Tribune Channel and at one location in Fyfe Sound (Figure 20). In each case, a plankton net (0.5 m diameter mouth, 2 m length, and 200 µ mesh size) with flow meter was towed horizontally at a depth of 1 to 2 m, very close to shore, and at a speed of 0.5 to 1 m s^{-1} against the prevailing current. These tows covered distances of several hundred meters and filtered volumes of water ranging from 8 to 90 m^3. The plankton samples were preserved and examined under a microscope at the Institute of Ocean Sciences, and the sea lice nauplii and copepodids identified and counted (Galbraith, 2005). In 17 of the 28 tows no lice were found, while in the remainder, copepodid concentrations ranged from 0.02 to 0.21 m^{-3}. Total volume of water filtered in the tows was 1,124 m^3, and the average copepodid concentration was 0.02 copepodids m^{-3}. A total of 24 planktonic larvae of *L. salmonis* were captured in the tows with 3 identified as nauplii and 21 as copepodids. Eleven of the copepodids were located less than 2 km away from a salmon farm and all three nauplii were within 0.1 km of a farm. The remaining 10 copepodids were located more than 3 km away from a salmon farm (Figure 20). Of the 28 plankton net tows, six were located adjacent to a farm site. The highest concentration (0.2 copepodids m^{-3}) and number of copepodids (6) were found in Fyfe Sound

near the Wicklow Point farm on March 29, 2008. Although the sample size of planktonic larvae was small and more limited in geographical extent, the model results were compared with the field observations. At the location in Fyfe Sound with the highest observed copepodid concentration, both the diel vertical migration and passive particle-tracking simulations predicted concentrations of ~10^{-2} copepodids m^{-3} (Figure 18), lower than the observed concentration of 2 × 10^{-1} copepodids m^{-3}. At other locations such as Hoeya Head, the simulated concentrations are several orders of magnitude lower than the observed concentrations of 0.1 m^{-3}. And at many locations where very low concentrations were predicted by the model, no copepodids were found in the plankton samples. Though our model predicted concentrations were consistently lower than the observed values, the spatial and temporal representativeness of the net tow sampling, species identification issues in the laboratory, and the relatively low numbers of captured larvae suggest large confidence limits around these field survey values. So although the relatively low model concentrations may be indicative of a systematic inaccuracy, such as strong nearshore velocities that flush the larvae out of the system too quickly (David Mackas, personal communication), it is difficult to be conclusive.

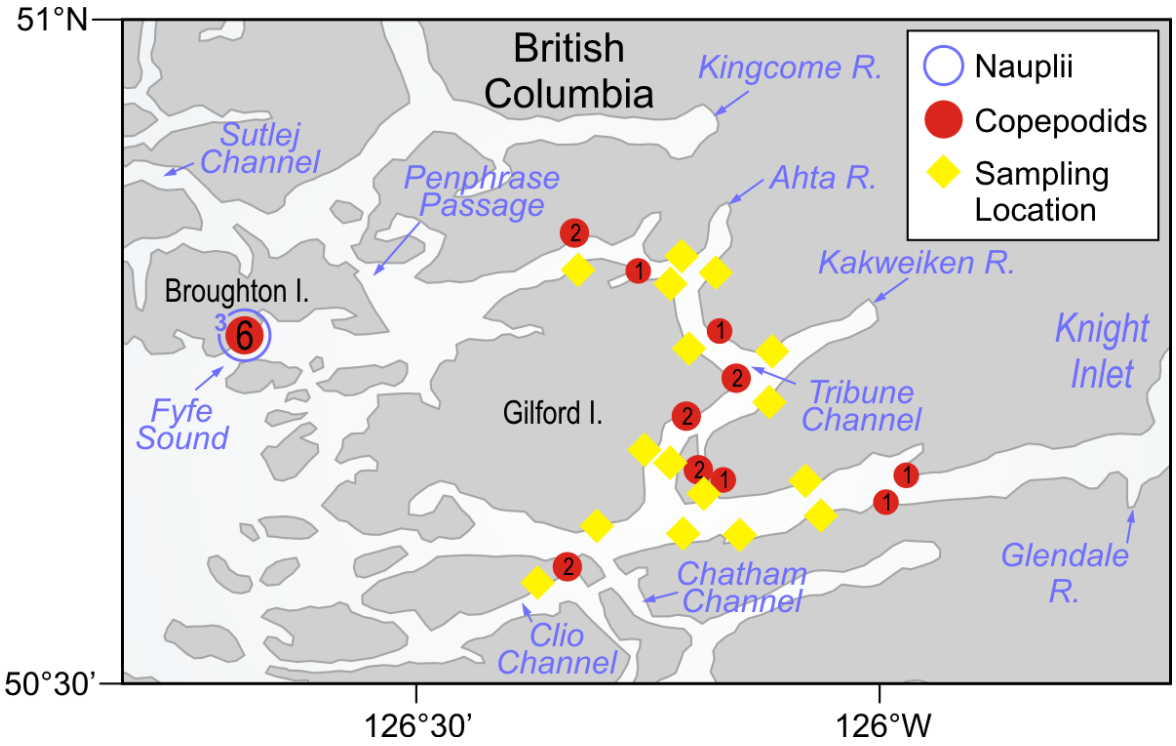

Figure 20. Location of plankton tows during the March 25 to 29, 2008 field survey. The number of copepodids caught in each tow is shown by the black number inside the red circle while the blue number next to a circle indicates the number of nauplii. Yellow diamonds denote sampling locations where no sea lice were caught.

Beach and purse seines have been used to capture wild fish during the outward migration season at locations throughout the Broughton Archipelago (Jones and Hargreaves, 2007, 2009). Subsamples of the catch of juvenile pink and chum salmon and other fish species were examined for sea lice (species, numbers, stage, and gender) and other metrics of the wild fish such as length and weight were also recorded. Almost all the juvenile pink and chum salmon collected in late March and early April 2008 were caught by beach seine in Knight Inlet (between Glendale Cove and the junction with Tribune Channel) and the southern portions of Tribune Channel. Very few juvenile pink and chum were caught in the northern and central regions of the Broughton Archipelago. No sea lice were found on any of the 342 juvenile pink

salmon examined (Jones and Hargreaves, 2009), and only two non-motile *L. salmonis* were found on the 263 juvenile chum salmon examined. The two juvenile chum salmon, each with one louse, were caught in the central Broughton region near the salmon farm at Cliffe Bay (Figure 2). A comparison between observed infestations on wild fish and predicted model copepodid concentrations is hampered by the skewed spatial distribution of the juvenile salmon, in which most fish were caught in Knight Inlet and Tribune Channel, combined with an almost complete absence of sea lice. However, the coincidence of very low copepodid concentrations predicted by our simulations and the very low infection levels in Knight Inlet and Thompson Sound is noteworthy. The two juvenile chum salmon with sea lice were netted in the central Broughton where our simulations predicted higher copepodid concentrations relative to those in Knight Inlet. These comparisons are also made difficult by the fact that the location of a beach survey which finds sea lice on juveniles does not mean that the sea lice attachment occurred at that same location. It could well have occurred upstream of the survey site. Though life stage of the sea louse may provide an estimate of time since the attachment, pinpointing the precise location of that attachment would also require information on the fish swimming speed and migration route. In short, there are uncertainties associated with using fish survey data to evaluate our model concentrations and to-date such comparisons have not been attempted.

Nevertheless, there have been discussions on doing this under the auspices of the Broughton Archipelago Monitoring Program (BAMP, a research program involving federal government, salmon farm producers, environmental non-governmental organizations and academic researchers. In particular, Stephanie Peacock, a Ph.D. student from the University of Alberta has suggested updating the fish monitoring analyses of Krkošek et al. (2005) by replacing their simple estimates of sea lice advection and dispersion with the sea lice concentration fields from our model tracking. A major achievement of BAMP has been the consolidation of the DFO and Krkošek sea lice-on-juvenile data sets into an online archive that should permit easier analysis. Two papers have already been published (Patanasatienkul et al. 2013; Rogers et al. 2013) on analyses of these combined data and more are planned.

4.3. RESULTS FROM THE DISCOVERY IHN$_V$ PARTICLE TRACKING MODEL

The IHNv particle tracking approach used in the Discovery Islands model is similar to that employed for sea lice in the Broughton Archipelago. Fifty particles were released randomly over a 100 m by 100 m by 10 m region that crudely represented a farm. This was done every hour for 11 days and each particle was tracked for 7 days. As with the sea lice, each particle represented a cohort of viruses whose precise number would be scaled-up later to be consistent with diseased fish shedding rates that were determined in laboratory experiments (Garver et al. 2013). The particles were then dispersed by the model currents and inactivated based on exposure to UV and background biota in the water. Surface UV values were based on weather station measurements and the (exponential) inactivation decay rate with depth was based on both laboratory tank and field measurements. The cumulative inactivation due to UV/biota was computed as the time integral of exposure over a prescribed time period.

Average viral concentrations over the top 10 m of the water column and over the period of 6 to 9 pm are shown in Figure 21 for April 12, 2010, 9 days after fictional disease outbreaks at one of 3 farms or 2 fish processing plants. Note that strong tidal currents in Discovery Passage mean a larger footprint for the processing plants located there. In particular, these footprints extend into the Strait of Georgia, not just further northward as would be the case if average surface estuarine flows were the only transport mechanism. Though not shown here, there is a time dependency not only due to the fluctuating tides and winds, but also due to daily periodicities in UV radiation. Specifically, the concentrations are larger just before dawn after the viruses have gone without exposure to UV radiation since the previous sunset.

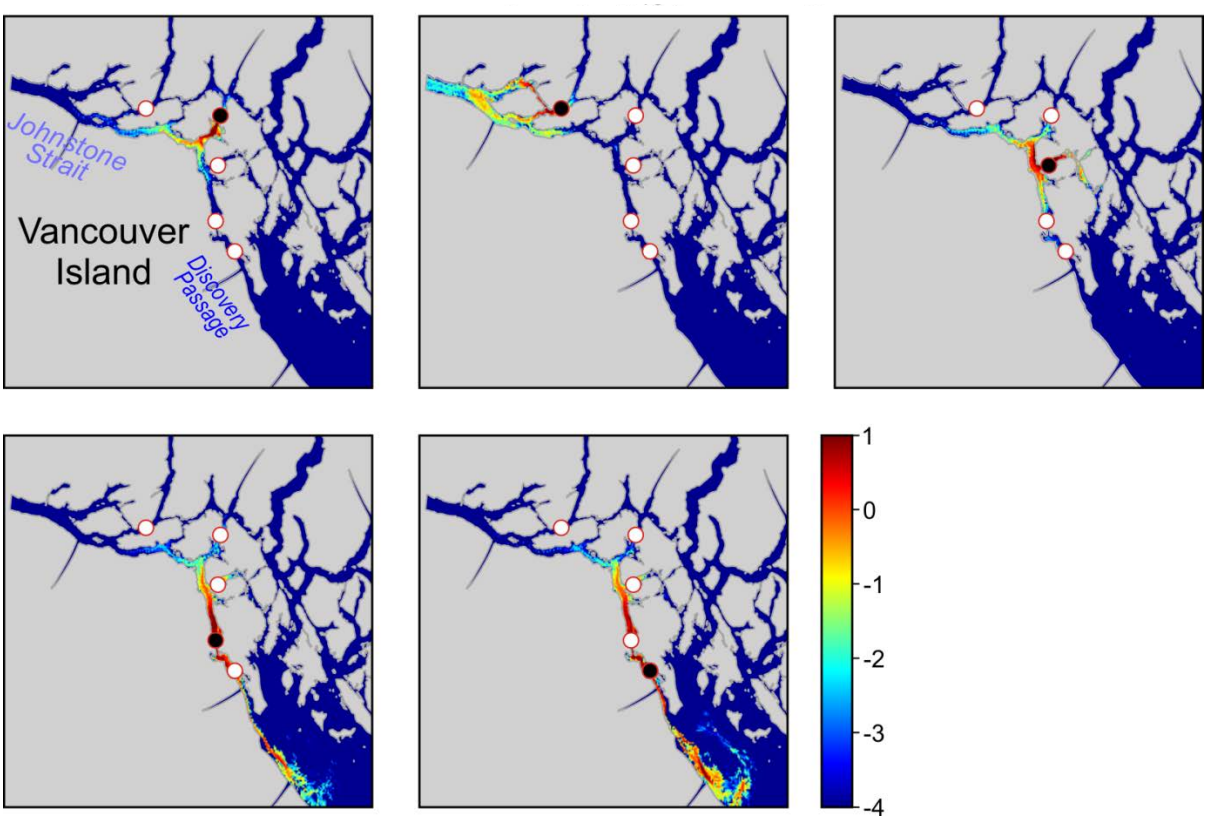

Figure 21. Hypothetical average IHN viral concentrations (log_{10}(viruses m^{-3})) over the top 10 m between the period of 6 to 9 pm on day 9 after the simulated disease outbreaks on April 12, 2010. The upper panels show the results based on an outbreak at each of three infected farms (black dots); the lower panels show the results based on an outbreak at each of two fish processing plants in Discovery Passage.

The outstanding question is whether viral concentrations arising from the water-borne transmission of an IHNv outbreak on one farm would be sufficient to infect a neighbouring farm. The answer requires monitoring the concentrations at neighbouring farms as a function of both time and depth to determine if they exceed the minimum infective dosage that would be needed to infect individual fish (Garver et al. 2013). This calculation will be carried out for potential disease outbreaks on all the Discovery farms but for now Figure 22b shows time-varying viral concentrations in the top 2 m of the water column at three farms (Nodales, Chancellor and Okisollo) based on the modelled release of 10^5 viruses every hour from the five surrounding farms. (Note that whereas Figure 21 gives a model-domain spatial snapshot at day 9, Figure 22 presents temporal variability at specific locations over the 18 day simulation.) Whereas the Chancellor and Okisollo farms show relatively small concentration levels from disease outbreaks at the other five farms, Nodales shows a much larger response, most of which comes from the nearby and upstream Owen Point farm.

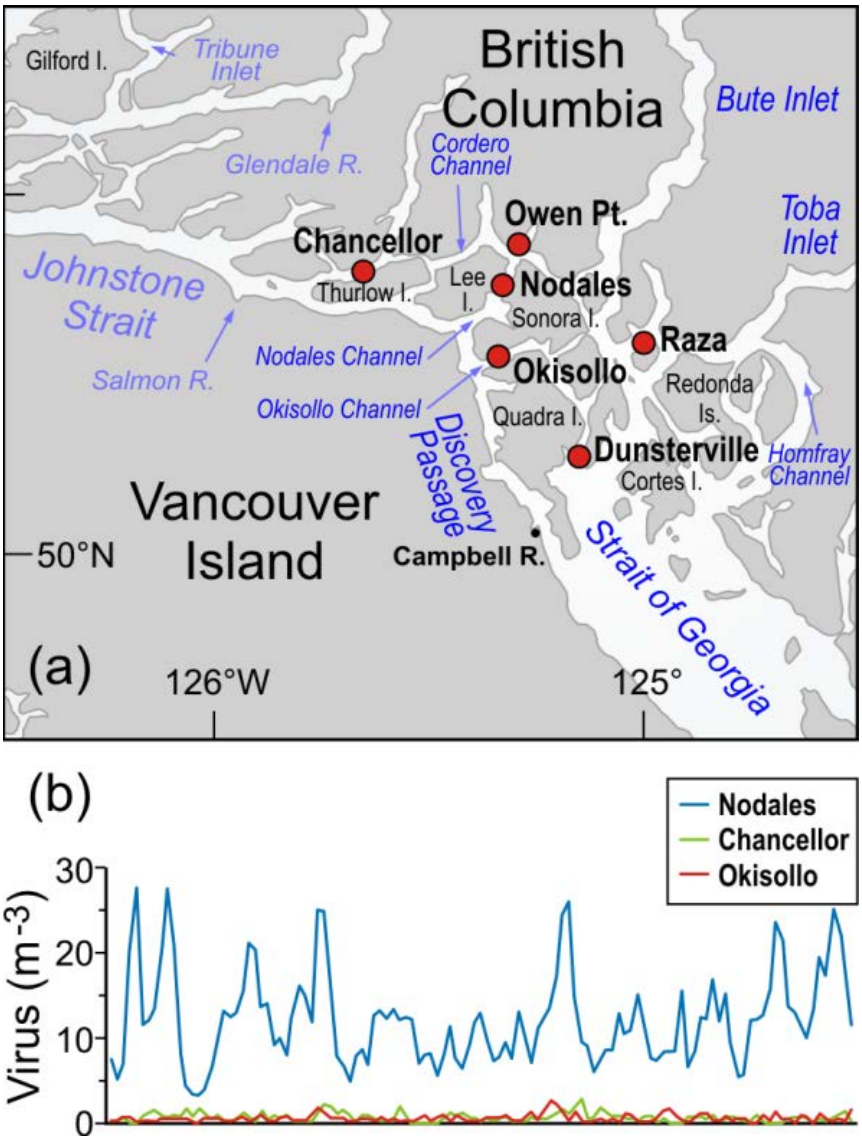

Figure 22. a) The six Discovery farms (red dots) for which the water-borne transport of fictitious IHNv disease outbreaks were simulated, b) time-varying viral concentrations in the top 2 m of the water column at three of those farms.

There are few available ways to evaluate the accuracy of these viral concentration field simulations. Were there a disease outbreak and sufficient resources to mount a field program that could measure the viral concentrations around the infected farm, then comparisons might be possible. This would assume the associated circulation model had sufficient forcing (e.g., atmospheric) and initial fields to produce velocity estimates for the required period of time. Another possibility would be simulating past outbreaks, such as those described in Saksida (2006). However in this case, the primary transmission vector was thought to be poor bio-security among workers travelling between farms. So model simulations that suggested water-borne transmission between farms would not be able to eliminate the possibility of other vectors.

5. APPLICATION TO AQUACULTURE SITING CRITERIA AND MANAGEMENT ZONES

In this section we attempt to address the fourth objective in the Terms of Reference for this document (Appendix A1), specifically, the identification of model outputs at the appropriate spatial and temporal resolutions that could be considered in the design of new and/or updated siting criteria and for the potential development of management zones for finfish aquaculture. Clearly, the particle tracking studies described earlier lend themselves to addressing the issue of dispersion of disease, parasites and pollutants from farms (or elsewhere) and thus could be useful in defining zones of influence and connectivity. In the following section, we will summarize some of the limitations or caveats that would be associated with providing that information, possible useful formats for presenting it, and possible future work.

5.1. CAVEATS AND LIMITATIONS

When using the output from coupled circulation and particle tracking models to define siting criteria and management zones, the following caveats and limitations should be kept in mind:

1) The physical oceanographic conditions in most coastal regions of British Columbia vary over a wide range of time scales. As FVCOM has only been run for relatively short time periods in specific years, it could be misleading to assume that the findings of those simulations are representative of all conditions. In particular, though tidal currents are generally quite regular and predictable, the wind driven and estuarine components of the current, and thus the dispersion patterns arising from them, can vary over a wide range of time scales. Similarly, water salinities and temperatures will also fluctuate and, as described earlier, will impact sea lice mortality and development. Though running our models for a wider range of conditions and using those results to estimate variability and uncertainty would be one way of addressing this issue, such an approach would require significant resources (personnel and computers) and a risk analysis could show it not to be worthwhile.

2) Not all particles have the same characteristics so that a “one size fits all” approach to management zones and/or siting may not be practical. Different species and pollutants will behave differently, may be subject to currents at different depths, and may need to be tracked for different periods of time. As their dispersion characteristics vary, so too does the modelling approach.

3) Model results are not perfect. Circulation model inaccuracies arise from a variety of reasons such as insufficient grid resolution, inaccurate forcing fields, inaccurate (e.g., smoothed) bathymetry, inaccurate numerical approximations to the governing (primitive) equations, inaccurate mixing and diffusion parameterizations, and physics not captured by the governing equations. Inaccuracies in the particle tracking model will arise from those in the circulation model fields and, if used, the random component, and the interval at which the FVCOM results are stored.

4) Though they might be considered a subset of the previous caveat, open (ocean) boundary conditions probably warrant mention in their own right. To date, all our circulation model simulations have employed open boundary conditions that are intended to allow outgoing signals to escape freely and have incoming salinities and temperatures remain relatively close to their climatological values. However, FVCOM has the provision to take these boundary conditions from the results of larger domain regional models like the Masson and Fine’s (2012) 1995-2002 hindcast of the BC shelf. Although this has yet to be done, it is planned. The boundary conditions adopted in the particle tracking model may also need re-visiting in light of possible inaccuracies they may be incurring. Recall that if a particle is

projected to cross a land, bottom, or open boundary in the next time step, it is held at the old location and will remain there until at some subsequent time the velocity moves it away from, rather than cross, that boundary. As such, except for those particles trying to escape from open boundaries few if any particles are permanently grounded. The fact that Figure 14 shows particles being trapped at the Johnstone Strait boundary in the Discovery grid indicates that open boundaries should be treated differently.

5) The transformation from particle positions to concentration fields presently requires defining a regular grid over the entire model domain and then computing densities. Although a finer regular grid should provide more accurate results, there is a trade-off with the number of particles that have been released. More releases should provide more accurate densities but will require more computer time. Alternative approaches, such as computing the densities on the triangular elements, or a cluster thereof, or using the offline dye concentration transport-diffusion code (as described below) need to be investigated.

5.2. POSSIBLE APPLICATION TO SITING AND MANAGEMENT ZONE DECISIONS

As seen in many of the figures and tables presented previously, there are a variety of ways to present the results of particle tracking experiments so they could assist in decision making for aquaculture siting and management. Animations showing individual particle positions or concentrations changing in time (e.g., Appendix A2) obviously provide nice visualizations, and particle snapshots (e.g., Figures 14, 18, 19, and 21) are also useful though, as noted before, some inaccuracies could be introduced in the transformation from particle positions. Connectivity tables (e.g., Table 2) can be used to summarize the likelihood of transmission between specific locations while transect-crossing vectors like those of Figure 15 provide a broader view of the routes taken. Of course, statistics on the average position and variability within a dispersion cloud (e.g., Figure 11 and Figures 46-52 in Page et al. 2013) can also be computed but in the complicated network of channels along the BC coast, those results could be more difficult to interpret than in more open regions.

In order to avoid the heavy cost of developing and maintaining operational models that could at any time, forecast the dispersion of particles and thus allow a manager to estimate potential transmission vectors, it would be possible to pre-compute a set of maps showing particle dispersion for a variety of seasonal (e.g., river discharge) and weather conditions. In addition to the variety of presentation formats shown and discussed already, it would not be difficult to adopt others (like GIS) that would allow flexibility in combining with other data.

5.3. RECOMMENDATIONS (ADVICE) AND FUTURE WORK

Given a) the uncertainties and caveats associated with the preceding model results, and b) the large investment in resources to develop and evaluate them, a primary question for aquaculture management division (AMD) is “Are the models now, or with some further development and evaluation, sufficiently useful tools to warrant the investment?” If the answer is no, then that should be the simple advice arising from this CSAS process and there is no need for further work. However, if the answer is yes (and we are assuming/hoping that will be the case) then it is useful to provide some guidance on what could be done next, both in terms of expanding the geographical coverage and model capabilities, and filling in what might be viewed as gaps in the existing work. The following list provides some thoughts on what that future work could entail.

1) The primary issue is whether more work is needed to enhance the credibility and/or utility of the existing Broughton and Discovery models and their results. Certainly much more could be done in terms of evaluating and enhancing model accuracy. In the Discovery Islands region there have been four more ADCP mooring deployments since the

publication of Foreman et al. (2012) and they could be used to further tune and evaluate both the original coarse, and newer, fine resolution models. Longer hindcasts that include heat flux forcing have also been carried out since the April 2010 simulation described in Foreman et al. (2012) and they should be evaluated against all available current, salinity and temperature observations. Similarly in the Broughton Archipelago, several FVCOM simulations have been carried out since the March 2008 hindcast described in Foreman et al. (2009) and they should be evaluated. As suggested by Figure 11, more work could also be done in exploring the sensitivity of the FVCOM storage interval to the subsequent convergence of the particle tracking results. The tracking period associated with the Figure 11 results was relatively short and it would be interesting to see how the convergence changes with longer tracking periods and releases in different parts of the model domain. However, further evaluation of the passive particle tracking results in both the Broughton and Discovery with, for example, more drifter studies would require more field work and the resources (personnel, ship-time) associated with such endeavours. The literature review summarized in section 1.2 indicates that with possible exception of SWNB, our evaluations are comparable to those that have been carried out in other regions of the world that employ models to help address aquaculture issues. However, whether our limited evaluations are deemed to be sufficient for local AMD is a question only they can answer.

2) Related to 1) is the limited temporal range of our hindcasts. Simulations prior to 2008 in the Broughton would, for example, allow studies on how the physical environment (salinity, temperature) might be related to large inter-annual variations in sea lice abundance (Patanasatienkul et al. 2013) and permit passive particle tracking evaluations against the GPS drifter studies carried out in 2006 and 2007. In addition to the usual personnel and computer resources that this work would require is the problem of assembling the necessary atmospheric forcing fields. Although our weather station network was not in place until 2008, preliminary work has been initiated to relate wind fields throughout the archipelago with observations at the Port Hardy airport which go back for decades. Needless to say, similar problems would exist for Discovery hindcasts prior to 2010, if for example, we wished to simulate water-borne transport during previous disease outbreaks. In this case, long weather records from the Campbell River airport could be useful.

3) Clearly more work could be done in exploring the potential for disease and parasite transfers from farms in the Discovery Islands to those in the Broughton Archipelago. (Although a more detailed examination is warranted, preliminary analyses suggest that due to generally northward and northwestward surface estuarine flows in the Discovery region, transfers from the Broughton to the Discovery are much less likely.) Although Figure 17 suggests this possibility with passive particles, there was a timing mismatch in the velocity fields, total transit times were not computed, and the effects of salinity, temperature, and UV radiation on biological (versus passive) particles were not taken into account.

4) A natural question associated with the previous issue is why we haven't joined the Broughton and Discovery model domains. Though this would certainly make it easier to investigate particle transfers between the two regions, it would also place higher demands on our computer resources, in terms of both the time and storage required to make the runs. It might also affect tidal accuracy as it is difficult to get the energy dissipation right in the Discovery portion and having values specified (i.e., constrained) in Johnstone Strait, rather than Queen Charlotte Sound, helps. Until the present IOS high performance

computer is upgraded or we have access to other more powerful systems, it is probably not feasible to consider joining the two grids.

5) As mentioned earlier, FVCOM now has an offline dye concentration module that might be preferable to the particle tracking module for computing and displaying the dispersion of fields (e.g., viruses, sea lice, pollutants) as it would avoid the conversion of particle densities into concentrations. Susan Haigh (personal communication) conducted some experiments with the analogous online version and found problems. It would be interesting to know if they also exist with the offline version. In a recent webinar presentation at the COMDA-sponsored FVCOM workshop, the FVCOM developers said that the new offline module should be more accurate.

6) There are many farms along the central and northwest coast of Vancouver Island (Figure 1) for which coupled circulation and dispersion models could be useful tools for aquaculture management. (There were disease outbreaks at farms in Clayoquot Sound in 2012.) In fact, in previous meetings with industry both Grieg and Mainstream have asked if such models could be developed. Though there are unstructured grids for this region, most have insufficient resolution up the inlets where the farms are located. So modifications would be needed. If this were to be done, then a parallel observational program would also be necessary to allow an adequate evaluation of the model accuracy. Needless to say, this would not be done quickly and appropriate resources (personnel, computing, instrumentation, ship time) would have to be allocated. Perhaps a cost benefit analysis on the pros-cons of using dispersion model results versus quicker estimates based on available or future current data needs to be carried out.

7) In a similar vein, there has been some discussion on relaxing the moratorium on aquaculture licensing and possible siting expansions to the central and north coast of BC. Here it would be possible to piggy-back on the high resolution FVCOM model that is being developed and evaluated as part of the “world class” project to assist with navigation and oil spill cleanups associated with increased tanker traffic coming into and leaving Kitimat. Note that this ocean circulation model development is being accompanied with the development (by EC) of high resolution weather and freshwater discharge models so it should have much better forcing fields than have been available in other regions. In fact, these new EC models may cover large portions of the province and thus could also be useful in the Broughton, Discovery, and west coast of Vancouver Island. If so, and weather hindcasts were performed and archived for past years, it would be interesting to use those data as forcing and both to compare results with previous output based on weather station and WSC forcing and, to assist in hindcasts such as those discussed in 2).

8) As mentioned earlier, several biological parameters are required as input to the sea lice and viral tracking models and although laboratory studies have provided some guidance on the required values or relationships, considerable uncertainty remains on both the specific values employed (as they are based on small statistical samples) and the applicability of relationships derived from laboratory studies to realistic oceanic conditions. As a consequence, there is also considerable uncertainty around the concentrations provided by our biological particle tracking models. Although future work to improve these parameters is clearly outside the expertise of hydrodynamic modellers, it should be done. That said, it would be valuable to use our models to conduct sensitivity studies to estimate the relative importance of all parameters and how critical the uncertainties are.

9) Throughout the development and application of our coupled hydrodynamic models and our participation in BAMP, contacts have been made with statistical and population

dynamics modellers and fisheries scientists outside of DFO. These have led to collaborations which have the potential to add further value to the modelling described here. For example

i. Erin Rees (UPEI) has been using our particle tracking results to investigate farm-to-farm transfer in the Broughton region and we believe, has plans to incorporate them into her population dynamics model.

ii. Stephanie Peacock, a PhD student at the University of Alberta, would like to modify the population dynamics models originally developed by Krkošek et al. (2005) by replacing their simple lice dispersion/advection component with lice concentrations that were computed by our models along potential juvenile salmon migration routes in the Broughton. The parameters in this model would be fit to sea lice-on-juvenile field data and among other things, provide estimates on where copepodids were most likely to have attached themselves to the wild juveniles.

iii. Scott Hinch and Nathan Furey (UBC) have developed an individual-based model wherein, analogous to Stephanie's, they would have a salmon swimming through Discovery Islands and encountering viruses (or sea lice) that our IHNv model has dispersed from one or more fictitious disease- (or sea louse-) infected farms. This work is in the very early stages but it may help in addressing some of Cohen's (2012) recommendations.

6. SUMMARY

The preceding presentation has provided a comprehensive summary of the development and application of hydrodynamic and particle tracking models to the dispersion of both passive and active particles originating on fish farms in the Broughton Archipelago and Discovery Islands. Model evaluations were presented along with assumptions, limitations and caveats associated with the model applications and interpretations of their results. Figure 23 summarizes the various components in developing, evaluating and interpreting the results from such models and notes both the section in which each is discussed, and the CSAS objective (Appendix 1) that is addressed.

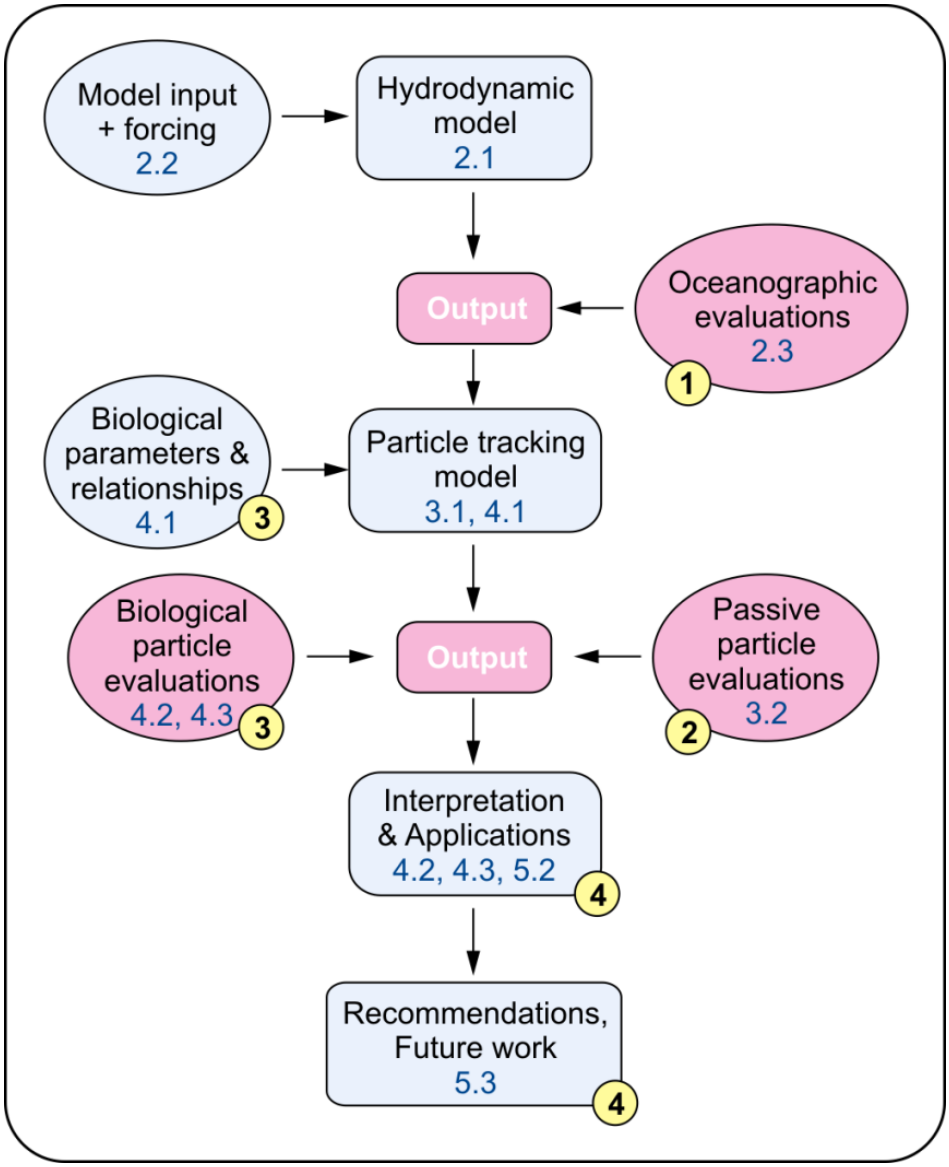

Figure 23. Schematic representation of the components required in the development, evaluation, and application of hydrodynamic and particle tracking models to the dispersion of particles from aquaculture facilities (adapted from Salama and Rabe 2013). Blue numbers within each bubble indicate the section where this topic is discussed while bubbles with grey shading denote those for which there are caveats, limitations and/or assumptions. The numbers within the yellow circles refer to objectives listed in the terms of reference for this document (Appendix 1).

7. ACKNOWLEDGMENTS

We thank Trish Kimber for assistance with many of the Figures; the local aquaculture industry (Marine Harvest Canada, Cermaq Canada, Grieg Seafoods) for their support and assistance with various field programs; members of BAMP for helpful discussions; the Program for Aquaculture Regulatory Research (PARR) and the Aquaculture Collaborative Research and Development Program (ACRDP) for their financial support; and the Centre for Ocean Model Development and Application (COMDA) for both financial and computing (the high performance computer at IOS) support.

8. REFERENCES

Asplin, L., Boxaspen, K.K., and Sandvik, A.D. 2011. Modelling the distribution and abundance of planktonic larval stages of *Lepeophtheirus salmonis* in Norway. *In* Salmon Lice: An integrated approach to understanding parasite abundance and distribution. Edited by S. Jones and R.J.Beamish. Wiley-Blackwell, Oxford. pp 31-50. (Accessed November, 2014)

Baker, P. and Pond, S. 1995. The low-frequency residual circulation in Knight Inlet, British Columbia. J. Phys. Oceanogr. 25; 747-763. (Accessed November 17, 2014)

Bennett, A.F. 2002. Inverse Modeling of the Ocean and Atmosphere. Cambridge University Press, Cambridge, U.K. 234 p.

Bricknell, I.R., Dalesman S., O'Shea, B., Pert, C.C., and Mordue, J. 2006. The effect of environmental salinity on sea lice (*Lepeophtheirus salmonis*) settlement success. Dis. Aquat. Organ. 71: 201–212.(Accessed November, 2014)

Brooks, K.M. 2005. The effects of water temperature, salinity and currents on the survival and distribution of the infective copepodid stage of sea lice (*Lepeophtheirus salmonis*) originating on Atlantic salmon farms in the Broughton Archipelago of British Columbia, Canada. Rev. Fish. Sci. 13: 177-204. (Accessed November 17, 2014)

Brooks, K.M. and Stucchi, D.J. 2006. The effects of water temperature, salinity, and currents on the survival and distribution of the infective copepodid stage of the salmon louse (*Lepeophtheirus salmonis*) originating on Atlantic salmon farms in the Broughton Archipelago of British Columbia, Canada (Brooks, 2005). A response to the rebuttal of Krkošek et al. (2005). Rev. Fish. Sci. 14: 13-23. (Accessed November 17, 2014)

Brooks, K.M. and Jones, S.R.M. 2008. Perspectives on pink salmon and sea lice: scientific evidence fails to support the extinction hypothesis. Rev. Fish. Sci. 16(4): 403-412. (Accessed November 17, 2014)

Canadian Tide and Current Tables. 2010. Discovery Passage and the West Coast of Vancouver Island, Volume 6. Fisheries and Oceans Canada, Ottawa. 131 p.

Chang, B.D., Page F.H., Losier R.J., Lawton P., Singh, R., and Greenberg, D.A. 2007. Evaluation of bay management area scenarios for the southwestern New Brunswick salmon aquaculture industry. Aquaculture Collaborative Research and Development Program final project report. Can. Tech. Rep. Fish. Aquat. Sci. 2722: 1-69.

Chen, C., Liu, H., and Beardsley, R.C. 2003. An unstructured, finite-volume, three-dimensional, primitive equation ocean model: application to coastal ocean and estuaries. J. Atmos. Ocean. Tech. 20: 159-186. (Accessed November 17, 2014)

Chen, C., Cowles, G. and Beardsley, R. C. 2004. An unstructured grid, finite-volume coastal ocean model: FVCOM User Manual. SMAST/UMASSD Technical Report-04-0601.

Chen, C., Beardsley, R.C., and Cowles, G. 2006a. An unstructured grid, finite-volume coastal ocean model (FVCOM) system. Oceanography, Special Issue on Advances in Computational Oceanography 19: 78-89. (Accessed November 17, 2014)

Chen, C., Beardsley, R.C., and Cowles, G. 2006b. An unstructured grid, finite-volume coastal ocean model. FVCOM user manual.

Chen, C., Beardsley, R.C., Cowles, G., Qi, J., Lai, Z., Gao, G., Stuebe, D., Xu, Q., Xue, P., Ge, J., Hu, S., Tian, R., Huang, H., Wu, L., and Lin, H. 2011. An Unstructured Grid, Finite-Volume Coastal Ocean Model FVCOM User Manual, Third edition. Marine Ecosystem Dynamics Modelling Laboratory, University of Massachusetts-Dartmouth, New Bedford, MA.

Cohen, B. I. 2012. The uncertain future of Fraser River sockeye: Commission of the Inquiry into the Decline of the Sockeye Salmon in the Fraser River, Public Works and Government Services Canada, Ottawa. 680 pp.

Foreman, M.G.G. 1984. A two dimensional dispersion analysis of selected methods for solving the linearized shallow water equations. J. Comput. Phys. 56: 287-323. (Accessed November 17, 2014)

Foreman, M.G.G., Stucchi, D.J., Zhang, Y., and A.M. Baptista. 2006. Estuarine and tidal currents in the Broughton Archipelago. Atmos Ocean. 44: 47-63. (Accessed November 17, 2014)

Foreman, M.G.G., Crawford, W.R., Cherniawsky, J.W., and Galbraith, J. 2008. Dynamic ocean topography for the Northeast Pacific and its continental margins. Geophys. Res. Lett. 35: L22606. (Accessed November 17, 2014)

Foreman, M.G.G., P. Czajko, P., Stucchi, D.J., and Guo, M. 2009. A finite volume model simulation for the Broughton Archipelago, Canada. Ocean Model. 30:29-47. (Accessed November 17, 2014)

Foreman, M.G.G., D.J. Stucchi, D.J., Garver, K.A., Tuele, D., Isaac, J., Grime, T., and Guo, M. 2012. A circulation model for the Discovery Islands, British Columbia. Atmos Ocean 50: 301-316. (Accessed November 17, 2014)

Galbraith, M.D. 2005. Identification of larval stages of *Caligus clemensi* and *Lepeophtheirus salmonis* from the Broughton Archipelago. Can. Tech. Rep. Fish. Aquat. Sci. 2548: 21 p.

Garver, K.A., Mahony, A.A.M.,Stucchi, D., Richard, J., Van Woensel, C., and Foreman, M.G.G. 2013. Estimation of Parameters Influencing Waterborne Transmission of Infectious Hematopoietic Necrosis Virus (IHNv) in Atlantic Salmon (*Salmo salar*). PLoS ONE 8 (12). (Accessed November 17, 2014)

Haney, R.L. 1991. On the pressure gradient force over steep topography in sigma coordinate ocean models. J. Phys. Oceanogr. 21: 610-619. (Accessed November 17, 2014)

Hayco. 2010. Wind observations in Douglas Channel, Squally Channel and Caamaño Sound. Technical Data Report for the Enbridge Northern Gateway Project, Vancouver.

Hayward, C.J., Andrews, M., and Nowak, B.F. 2011. Introduction: *Lepeophtheirus salmonis* – A remarkable success story. *In* Salmon Lice: An Integrated Approach to Understanding Parasite Abundance and Distribution. Edited by S. Jones and R.J.Beamish. Wiley-Blackwell, Oxford. pp 1-28. (Accessed November 17, 2014)

Henry, R.F., and Walters, R.A.1993. A geometrically-based, automatic generator for irregular triangular networks. Commun. Numer. Meth. En. 9: 555-566. (Accessed November 17, 2014)

Heuch, P.A., Nordhagen, J.R., and Schram, T.A. 2000. Egg production in the salmon louse [*Lepeophtheirus salmonis* (Krøyer)] in relation to origin and water temperature. Aquacult. Res. **31**: 805-814. (Accessed November 17, 2014)

Johnson, S.C. and Albright, L.J. 1991. *Development, growth and survival of Lepeophtheirus salmonis* (Copepoda: Caligidae) under laboratory conditions. J. Mar. Biol. Assoc. UK. 71: 425-436. (Accessed November 17, 2014)

Jones, S.R.M. and Hargreaves, N.B. 2007. The abundance and distribution of *Lepeophtheirus salmonis* (Copepoda: Caligidae) on pink *Oncorhynchus gorbuscha* and chum *O. keta* salmon in coastal British Columbia. J. Parasit. 93: 1324-1331. (Accessed November 17, 2014)

Jones, S.R.M. and Hargreaves, N.B. 2009. Infection threshold to estimate *Lepeophtheirus salmonis*-associated mortality among juvenile pink salmon. Dis. Aquat. Organ. 84: 131–137. (Accessed November 17, 2014)

Krkošek, M., Lewis, M.A., and Volpe, J.P., 2005. Transmission dynamics of parasitic sea lice from farm to wild salmon. Proc. R. Soc. B. 272, 689-696. (Accessed November, 2014)

Krkošek, M., Ford, J.S., Morton, A., Lele, S., Myers, R.A., and Lewis, M.A., 2007. Declining wild salmon populations in relation to parasites from farm salmon. Science. 328: 1772-1775. (Accessed November 17, 2014)

Masson, D., and I. Fine. 2012. Modeling seasonal to inter-annual ocean variability of coastal British Columbia,. J. Geophys. Res. 117, C10019.

Navas, J.M., Telfer, T.C., and L.G. Ross, L.G. 2011. Application of 3D hydrodynamic and particle tracking models for better environmental management of finfish culture. Cont. Shelf Res. 31: 675-684. (Accessed November 17, 2014)

Page, F., Chang, B.D., Beattie, M., Losier, R., McCurdy, P., Bakker, J., Haughn, K., Thorpe, B., Fife, J., Scouten, S., Bartlett, G., and Ernst, B. 2014. Transport and dispersal of sea lice bath therapeutants from salmon farm net-pens and well-boats operated in Southwest New Brunswick: a mid-project perspective and perspective for discussion. DFO Can. Sci. Advis. Sec. Res. Doc. 2014/102. v + 63 p. (Accessed November 17, 2014)

Patanasatienkul, T., J. Sanchez, J., Rees, E.E., Krkošek, M., Jones, S.R.M., and Revie, C.W. 2013. Sea lice infestations on juvenile chum and pink salmon in the Broughton Archipelago, Canada from 2003 to 2012. Dis. Aquat. Org. 105:149-161. (Accessed November 17, 2014)

Peterman, R.M., Marmorek, D., Beckman B., Bradford, M., Mantua, N., Riddell, B., Scheuerell, M., Staley, M., Wieckowski, K., Winton, J., and Wood, C.. 2010. Synthesis of evidence from a workshop on the decline of Fraser River Sockeye. June 15-17, 2010. A Report to the Pacific Salmon Commission. 123 pp.

Price, M.H.H., Morton, A., and Reynolds, J.D. 2010. Evidence of farm-induced parasite infestations on wild juvenile salmon in multiple regions of coastal British Columbia, Canada. Can. J. Fish. Aquat. Sci. 67: 1925-1932.(Accessed November 17, 2014)

Rogers, L.A., Peacock, S.J., McKenzie, P., DeDominicis, S., Jones, S.R.M., Chandler, P., Foreman, M.G.G., Revie, C.W. and Krkošek, M. 2013. Modeling Parasite Dynamics on Farmed Salmon for Precautionary Conservation Management of Wild Salmon. *PLoS ONE* 8(4). (Accessed November 17, 2014)

Salama, N.K.G., Collins, C.M., Fraser, J.G., Dunn,J., Pert, C.C., Murray, A.G., and Rabe, B. 2013. Development and assessment of a biophysical dispersal model for sea lice. J. Fish. Dis. 36: 323−337. (Accessed November 17, 2014)

Salama, N.K.G., and Rabe, B. 2013. Developing models for investigating the environmental transmission of disease-agents with open-cage salmon aquaculture, Aquacult. Env. Interact. 4: 91-115. (Accessed November 17, 2014)

Saksida, S.M. 2006. Infectious haematopoietic necrosis epidemic (2001 to 2003) in farmed Atlantic salmon *Salmo salar* in British Columbia. Dis. Aquat. Org. 72: 213-223. (Accessed November 17, 2014)

Stien, A., Bjørn, P.A., Heuch, P.A., and Elston, D. A. 2005. Population dynamics of salmon lice *Lepeophtheirus salmonis* on Atlantic salmon and sea trout. Mar. Ecol-Prog Ser. 290: 263–275. (Accessed November 17, 2014)

Stucchi, D., Guo, M., Foreman, M.G.G., Czajko, P., Galbraith, M., Mackas, D. L., and Gillibrand, P.A. 2011. Modelling sea lice production and concentrations in the Broughton Archipelago, British Columbia. *In* Salmon Lice: An integrated approach to understanding parasite abundance and distribution. Edited by S. Jones and R.J.Beamish. Wiley-Blackwell, Oxford. pp 117-150. (Accessed November 17, 2014)

Thomson, R.E. 1981. Oceanography of the British Columbia Coast. Can. Spec. Pub. Fish. Aquat. Sci. 56. 291 p.(Accessed November, 2014)

Wahba, G. 1990. Spline models for observational data. Vol. 59 in the CBMS-NSF Regional Conference Series in Applied Mathematics. SIAM, Philadelphia, USA. 169 p.

Wu, Y., J. Chaffey, B. Law, D.A. Greenberg, A. Drozdowski, F. Page, and S. Haigh. 2014. A three-dimensional hydrodynamic model for aquaculture: a case study in the Bay of Fundy. Aquacult. Environ. Interact. 5: 235-248.